

Stochastic symplectic ice

Chenyang Zhong ^{*}

January 31, 2021

Abstract

In this paper, we construct solvable ice models (six-vertex models) with stochastic weights and U-turn right boundary, which we term “stochastic symplectic ice”. The models consist of alternating rows of two types of vertices. The probabilistic interpretation of the models offers novel interacting particle systems where particles alternately jump to the right and then to the left. Two colored versions of the model and related stochastic dynamics are also introduced. Using the Yang-Baxter equations, we establish functional equations and recursive relations for the partition functions of these models. In particular, the recursive relations satisfied by the partition function of one of the colored models are closely related to Demazure-Lusztig operators of type C.

1 Introduction

Since the pioneering investigation by Baxter ([1],[2]), exactly solvable lattice models have found applications to various fields of mathematics and mathematical physics. “Exactly solvable” means that the Yang-Baxter equation, or “star-triangle relation”, is satisfied by the system. We refer the reader to [28],[10],[23],[24] for applications of exactly solvable models to many algebraic combinatorics problems.

Recently, there has been a series of work (see, for example, [13],[11],[6],[9],[7],[8]) relating representation theory (for example, Tokuyama-type formulas and non-archimedean Whittaker functions) to exactly solvable lattice models. These models are for Cartan type A, and are based on the Yang-Baxter equation for free Fermionic six-vertex models ([13]).

For Cartan type C, a parallel line of work has been initiated by Hamel and King ([20],[21]) and Ivanov ([22]). These works showed that the partition function of certain ice model (six-vertex model) equals the product of a deformation of Weyl’s denominator and an irreducible character of the symplectic group $\mathrm{Sp}(2n, \mathbb{C})$. Ivanov’s approach used the Yang-Baxter equation developed in [13]. His lattice model consists of alternating rows of two types of ice (called Γ ice and Δ ice) and has U-turn boundary on the right end. This U-turn type model was also applied to Whittaker functions on the metaplectic double cover of $\mathrm{Sp}(2n, F)$ where F is a non-archimedean local field ([12]). Later work ([19]) extended the results to metaplectic ice for Cartan type C. In [15], new deformations of Weyl’s character formula for Cartan type B,C and D, and a character formula of Proctor for type BC, were obtained using the Yang-Baxter equation. A different approach based on a discrete time evolution operator on one-dimensional Fermionic Fock space is in [16]. Further developments, including dual wave function of the symplectic ice and generalizations of the ice models in [22] and [12], are in [25],[26].

Another sequence of recent work, which comes from the subject of “integrable probability”, relates stochastic systems such as the asymmetric simple exclusion processes (ASEP) and the KPZ equation, to solvable lattice models called the stochastic higher spin six-vertex models (see, for example, [3],[18]). Exactly solvable lattice models provide a powerful tool for analyzing probabilistic properties of these stochastic systems (for example, for proving Tracy-Widom type fluctuation results). The reader is also referred to [4] for a useful tutorial. The works on stochastic vertex models so far have been mainly restricted to models that are related to Cartan type A.

^{*}Department of Statistics, Stanford University

The focus of this paper is to provide the first stochastic model for Cartan type C, which we term “stochastic symplectic ice”. This serves as an attempt to connect the above two sequences of work. Specifically, we construct two types of ice models (six-vertex models) with stochastic weights and U-turn boundary on the right end. The difference between the two types of models lies in the boundary condition at the U-turns (reflecting, or absorbing-and-emitting, see Section 2.1 for details). The rows of the model alternate with two types of vertices, which we term “stochastic Γ vertex” and “stochastic Δ vertex”, in analogy to the terms used for Ivanov’s model. The model shares some features with Ivanov’s symplectic ice model, but the Boltzmann weights are quite different from previous works.

The stochastic symplectic ice model also offers novel stochastic dynamics for interacting particle systems. Under the probabilistic interpretation, the particles alternately jump to the right and then jump to the left. The particles are reflected from the U-turn boundary, or absorbed into/emitted from the U-turn (depending on the type of the model). The partition function represents the probability of obtaining a particular particle configuration at the end of the evolution.

The models are solvable, in that they satisfy the Yang-Baxter equation. In fact, four sets of Yang-Baxter equations are found for these models. Combining the Yang-Baxter equations with two further relations, the caduceus relation and the fish relation, we derive functional equations for both models (see Theorem 2.3).

A recent work by Borodin and Wheeler introduced a new attribute called “color” to stochastic vertex models ([5]). The colored stochastic vertex models are related to the quantum group $U_q(\widehat{\mathfrak{sl}_{n+1}})$, and degenerate to multi-species versions of interacting particle systems (such as multi-species ASEP). In [5], recursive relations for the partition functions of these colored models were derived using the Yang-Baxter equation, and were related to Demazure-Lusztig operators (of type A).

In this paper, we also construct two colored versions of the stochastic symplectic ice model. The colored models are also stochastic, and can be interpreted as stochastic dynamics of interacting particles with colors. In one of the colored models (which we introduce and study in Section 3), each particle carries a “signed color”, whose sign changes to the opposite when reflected from the U-turn boundary. This seems to be a novel feature compared to previous colored stochastic vertex models. When specifying the boundary conditions, two signed permutations from the hyperoctahedral group (which is the Weyl group for type C) are involved. Previous works have mainly been focusing on boundary conditions specified by the symmetric group (which is the Weyl group for type A).

The colored models are also solvable, in that three sets of the Yang-Baxter equations are satisfied by the models. These equations, when combined with a further relation, the reflection equation, allow us to obtain recursive relations for the partition functions. The recursive relations for one of the colored models are further related to Demazure-Lusztig operators of type C.

A few days before this paper is posted, a preprint by Buciumas and Scrimshaw ([17]) appeared on the arXiv. Their work constructed colored lattice models with partition functions representing symplectic and odd orthogonal Demazure characters and atoms. The work in this paper was done independently of and concurrently with their work. We also note that the colored models in this paper are quite different from theirs: the colored models in this paper are six-vertex models, while their models are five-vertex models (in that the b_1 patterns for both Γ ice and Δ ice have Boltzmann weight 0 in their paper); the Boltzmann weights in this paper are also quite different from theirs; the recursive relations in this paper are related to Demazure-Lusztig operators of type C, while theirs are related to Demazure atoms and characters.

Section 2 of the paper introduces the two types of the stochastic symplectic ice model. The Yang-Baxter equations, the caduceus relation and the fish relation are presented there. These relations are used to derive the functional equations for the partition functions. Section 3 introduces one of the colored models for the stochastic symplectic ice. The Yang-Baxter equations and the reflection equation are also introduced in this section. Using these relations, the recursive relations for the partition functions are obtained. The recursive relations are further related to Demazure-Lusztig operators of type C. Finally we introduce and study the other colored model in Section 4.

a_1	a_2	b_1	b_2	c_1	c_2
1	1	z_i	qz_i	$1 - qz_i$	$1 - z_i$

Figure 1: Boltzmann weights for stochastic Γ vertex with spectral parameter z_i

1.1 Acknowledgement

The author wishes to thank Daniel Bump for his encouragement and many helpful conversations.

2 Stochastic symplectic ice

In this section, we introduce and study two classes of stochastic symplectic ice. They are termed “reflecting stochastic symplectic ice” and “absorbing-and-emitting stochastic symplectic ice”. Section 2.1 introduces the models and related Boltzmann weights. Section 2.2 gives the Boltzmann weights for the R-matrices and shows the Yang-Baxter equation. An additional relation, the “caduceus relation”, is shown in Section 2.3. By combining the Yang-Baxter equation with the caduceus relation and a further relation, the “fish relation”, we establish functional equations satisfied by the partition functions in Section 2.4.

2.1 The models

First we introduce some notations. By “ice model”, we mean a planar lattice where every edge is assigned a $+$ or $-$ spin. To each vertex in the lattice, we assign a Boltzmann weight, which is a number that depends on the type of the vertex (there are two types of vertices for stochastic symplectic ice, see the next paragraph) and the $+$ or $-$ spins assigned to the four adjacent edges. A configuration/state means a labeling of the edges of the graph by $+$ or $-$ spins, and the Boltzmann weight of a configuration is the product of the Boltzmann weights of all the vertices for the configuration. An admissible state is a state where the assignment of spins to the edges adjacent to each vertex is one of the allowed assignments for that vertex (the allowed assignments are listed in tables later in the paper). The partition function of the ice model is the sum of Boltzmann weights for all admissible configurations.

In the stochastic symplectic ice model, two types of vertices are involved. They are termed “stochastic Γ vertex” and “stochastic Δ vertex” in this paper, in analogy to the Γ ice and the Δ ice used in Ivanov’s symplectic ice model (see [22]). The model depends on $n + 1$ parameters z_1, \dots, z_n, q , where z_1, \dots, z_n are called “spectral parameters” and q is called “deformation parameter”. Throughout the paper, we also define

$$z'_i = q + 1 - \frac{1}{z_i},$$

for every $1 \leq i \leq n$.

The Boltzmann weights for the stochastic Γ vertex and the stochastic Δ vertex (with spectral parameter z_i) are listed in Figures 1-2. Throughout the paper, an assignment of spins to the adjacent edges of a vertex that is not listed in the corresponding table has Boltzmann weight 0.

Now we introduce the stochastic symplectic ice model. We consider a rectangular lattice with $2n$ rows and L columns. The rows are numbered $1, 2, \dots, 2n$ from bottom to top, and the columns are numbered $1, 2, \dots, L$ from right to left. Every odd-numbered row is a row of stochastic Δ vertices, and every even-numbered row is a row of stochastic Γ vertices. The spectral parameter for the i th row of stochastic Γ vertices and the i th row of stochastic Δ vertices is given by z_i .

a_1	a_2	b_1	b_2	d_1	d_2
1	1	z'_i	$\frac{1}{q}z'_i$	$1 - z'_i$	$1 - \frac{1}{q}z'_i$

Figure 2: Boltzmann weights for stochastic Δ vertex with spectral parameter z_i , where $z'_i = q + 1 - \frac{1}{z_i}$

The model also depends on a partition $\lambda = (\lambda_1, \dots, \lambda_{n'}) \in \mathbb{Z}^{n'}$, where $\lambda_1 \geq \dots \geq \lambda_{n'}$ and $n' \in \mathbb{N}_+$. We assume that $L \geq \lambda_1 + n'$. The assignment of spins to boundary edges of the rectangular lattice is given as follows: on the left column, we assign $-$ to each row of stochastic Γ vertex, and $+$ to each row of stochastic Δ vertex; on the top, we assign $+$ to each boundary edge; on the bottom, we assign $-$ to each column labeled $\lambda_i + n' + 1 - i$, for $1 \leq i \leq n'$; on the right, the i th row of stochastic Γ vertices and the i th row of stochastic Δ vertices is connected by a “cap”.

For example, when $n = 2$, $\lambda = (2, 1)$, $L = 4$, the model configuration is shown in Figure 3.

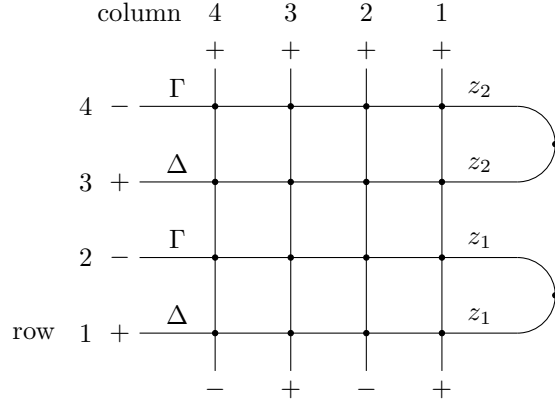


Figure 3: Model configuration when $n = 2, \lambda = (2, 1), L = 4$

We now discuss the Boltzmann weights for the caps. There are two choices of Boltzmann weights for the caps, which lead to two types of stochastic symplectic ice: “reflecting stochastic symplectic ice” and “absorbing-and-emitting stochastic symplectic ice”. The Boltzmann weights of the caps for the two models are listed in Figures 4-5, respectively. For reflecting symplectic ice, we always assume that $n' = n$ when taking the partition λ for boundary conditions (by particle conservation).

Cap		
	1	1

Figure 4: Boltzmann weights for caps: reflecting stochastic symplectic ice

Throughout the paper, we denote by $z = (z_1, z_2, \dots, z_n)$ the vector of the n spectral parameters. We also denote by $\mathcal{S}_{n,L,\lambda,z}$ the collection of admissible configurations of the reflecting symplectic ice with $2n$

Cap		
	1	1

Figure 5: Boltzmann weights for caps: absorbing-and-emitting stochastic symplectic ice

rows, L columns, spectral parameters z_1, \dots, z_n and bottom boundary condition given by λ . We also let $Z(\mathcal{S}_{n,L,\lambda,z})$ be the corresponding partition function. The collection of admissible configurations and the partition function of the absorbing-and-emitting stochastic symplectic ice are denoted by $\mathcal{T}_{n,L,\lambda,z}$ and $Z(\mathcal{T}_{n,L,\lambda,z})$, respectively.

We note that the Boltzmann weights of our model are stochastic. For stochastic Γ vertex, we view the left and top edges adjacent to the vertex as input, and the other two as output; for stochastic Δ vertex, we view the right and top edges adjacent to the vertex as input, and the other two as output; for caps, we view the top spin as input and the bottom spin as output. It can be seen that the possible Boltzmann weights for a given vertex (either the stochastic Γ vertex, the stochastic Δ vertex or the cap) with given input sum up to 1. Moreover, if z satisfies the condition

$$\max\{0, \frac{1}{q+1}\} \leq z_i \leq \min\{\frac{1}{q}, 1\}, \text{ for every } 1 \leq i \leq n, \quad (2.1)$$

then all possible Boltzmann weights are non-negative. Therefore, when the condition (2.1) is satisfied, the Boltzmann weight of a given vertex can be interpreted as the probability of obtaining the output given the input at that vertex.

We also note that if the condition (2.1) is satisfied by z , then both types of stochastic symplectic ice can be interpreted as an interacting particle system. We put $x - y$ coordinates on the rectangular lattice (see, for example, Figure 3) such that the x coordinate of the i th row is i and the y coordinate of the j th column is j . For each $t = 0, 1, \dots, 2n$, we consider the set of vertical edges of the lattice that have a non-empty intersection with the line $x = 2n - t + \frac{1}{2}$ and carry a $-$ spin. The positions of the particles at time t are just the y coordinates of these vertical edges. Therefore, an admissible state of the stochastic symplectic ice gives a possible evolution of the particles, and the Boltzmann weight for that state represents the probability of the particular evolution.

Now we describe the stochastic dynamics of the particles. For $t = 0, 1, \dots, 2n - 1$, if t is even, the particles attempt to jump to the right; if t is odd, the particles attempt to jump to the left.

The detailed rule is as follows. When t is even, the particles are ordered from left to right. There is a new particle entering from the left boundary (we call it 0th particle), which jumps to the right with geometric jump size (with parameter $qz_{n-\frac{t}{2}}$) unless it hits the 1st particle; if the particle hits the 1st particle, then it stops to move further. Starting from $l = 1$, if the l th particle wasn't hit by any particle on its left, we flip a coin with head probability $z_{n-\frac{t}{2}}$ to determine whether it will stay at its current position or not; if the coin comes up tail, then the particle jumps to the right with geometric jump size (with parameter $qz_{n-\frac{t}{2}}$) unless it hits the $(l+1)$ th particle; if the particle hits the $(l+1)$ th particle, then it stops to move further. If the l th particle was hit by the $(l-1)$ th particle, it jumps to the right by 1 and the following move is the same as the previous case (except for the first step determining whether it will stay at the current position). Then the $(l+1)$ th particle begins to move. If the rightmost particle moves beyond the first column (meaning that it hits the cap), for reflecting symplectic ice it is reflected by the cap (so it will start to move leftward from the first column at time $t+1$), while for absorbing-and-emitting symplectic ice it is absorbed. For absorbing-and-emitting symplectic ice, if no particle hits the cap, a new particle will be emitted from the first column at time $t+1$.

When t is odd, the particles are ordered from right to left. If there is a particle reflected/emitted from the cap (we call it 0th particle), it jumps to the left with geometric jump size (with parameter $\frac{1}{q}z'_{n-\frac{t-1}{2}}$)

unless it hits the 1st particle; if the particle hits the 1st particle, then it stops to move further. Starting from $l = 1$, if the l th particle wasn't hit by any particle on its right, we flip a coin with head probability $z'_{n-\frac{t-1}{2}}$ to determine whether it will stay at its current position or not; if the coin comes up tail, then the particle jumps to the left with geometric jump size (with parameter $\frac{1}{q}z'_{n-\frac{t-1}{2}}$) unless it hits the $(l+1)$ th particle; if the particle hits the $(l+1)$ th particle, then it stops to move further. If the l th particle was hit by the $(l-1)$ th particle, it jumps to the left by 1 and the following move is the same as the previous case (except for the first step determining whether it will stay at the current position). Then the $(l+1)$ th particle begins to move.

Under this probabilistic interpretation, the partition functions $Z(\mathcal{S}_{n,L,\lambda,z})$ and $Z(\mathcal{T}_{n,L,\lambda,z})$ represent the probability that the particle configuration at time $t = 2n$ corresponds to the partition λ (meaning that the i th particle, ordered from left to right, has coordinate $\lambda_i + n' + 1 - i$ for $1 \leq i \leq n'$) and no particle has ever moved left of the L th column.

2.2 The R-matrix and the Yang-Baxter equation

The Yang-Baxter equation is a powerful tool for studying solvable lattice models. It involves two ordinary vertices (for our model, the stochastic Γ vertex or the stochastic Δ vertex) and one additional rotated vertex called the R-vertex (also called the “R-matrix”, due to connections to quantum group theory).

The stochastic symplectic ice, as introduced in Section 2.1, is a solvable lattice model, in that we can find four types of R-matrices such that four sets of Yang-Baxter equations are satisfied by the model. In this section, we introduce the R-matrices for the stochastic symplectic ice, and show that the R-matrices together with the ordinary vertices (stochastic Γ and Δ vertex) satisfy the Yang-Baxter equations, in the form of Theorem 2.1 below.

The four types of R-matrices are termed “stochastic $\Gamma - \Gamma$ vertex”, “stochastic $\Gamma - \Delta$ vertex”, “stochastic $\Delta - \Delta$ vertex” and “stochastic $\Delta - \Gamma$ vertex”, in analogy to the terms used in [22] for the symplectic ice. The Boltzmann weights for these R-matrices are given in Figures 6-9.

1	1	$\frac{z_i - z_j}{1 - (q+1)z_j + qz_i z_j}$	$\frac{q(z_i - z_j)}{1 - (q+1)z_j + qz_i z_j}$	$\frac{(1 - qz_i)(1 - z_j)}{1 - (q+1)z_j + qz_i z_j}$	$\frac{(1 - z_i)(1 - qz_j)}{1 - (q+1)z_j + qz_i z_j}$

Figure 6: Boltzmann weights for stochastic $\Gamma - \Gamma$ vertex with spectral parameters z_i and z_j

1	1	$\frac{z'_i + qz_j - (q+1)z'_i z_j}{1 - z'_i z_j}$	$\frac{q^{-1}z'_i + z_j - (1 + q^{-1})z'_i z_j}{1 - z'_i z_j}$	$\frac{(1 - z'_i)(1 - qz_j)}{1 - z'_i z_j}$	$\frac{(1 - q^{-1}z'_i)(1 - z_j)}{1 - z'_i z_j}$

Figure 7: Boltzmann weights for stochastic $\Delta - \Gamma$ vertex with spectral parameters z_i and z_j

The following theorem gives the four sets of Yang-Baxter equations for the stochastic symplectic ice.

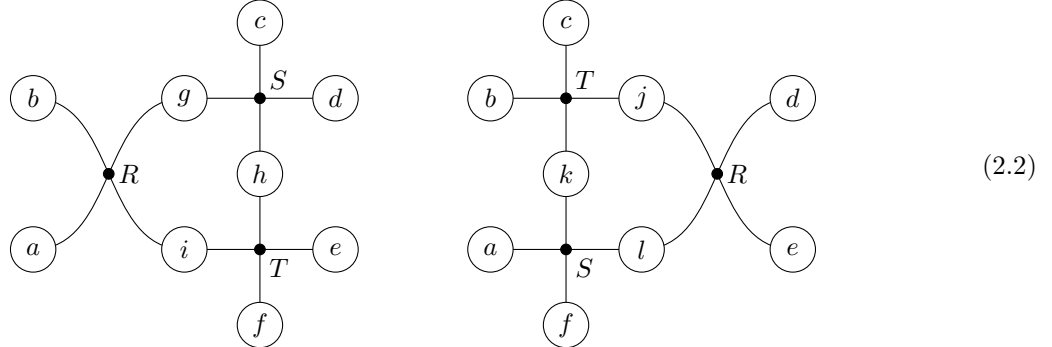
1	1	$\frac{z'_j - z'_i}{q - (q+1)z'_i + z'_i z'_j}$	$\frac{q(z'_j - z'_i)}{q - (q+1)z'_i + z'_i z'_j}$	$\frac{(1-z'_i)(q-z'_j)}{q - (q+1)z'_i + z'_i z'_j}$	$\frac{(1-z'_j)(q-z'_i)}{q - (q+1)z'_i + z'_i z'_j}$

Figure 8: Boltzmann weights for stochastic $\Delta - \Delta$ vertex with spectral parameters z_i and z_j

1	1	$\frac{qz_i + z'_j - (1+q)}{z_i z'_j - 1}$	$\frac{qz_i + z'_j - (1+q)}{q(z_i z'_j - 1)}$	$\frac{(1-qz_i)(1-z'_j)}{z_i z'_j - 1}$	$\frac{(1-z_i)(q-z'_j)}{q(z_i z'_j - 1)}$

Figure 9: Boltzmann weights for stochastic $\Gamma - \Delta$ vertex with spectral parameters z_i and z_j

Theorem 2.1. For any $X, Y \in \{\Gamma, \Delta\}$ the following holds. Assume that S is stochastic X vertex with spectral parameter z_i , T is stochastic Y vertex with spectral parameter z_j , and R is stochastic $X - Y$ vertex with spectral parameters z_i, z_j . Then the partition functions of the following two configurations are equal for any fixed combination of spins a, b, c, d, e, f .



Proof. There are in total $2^6 = 64$ possible combinations of the boundary spins a, b, c, d, e, f . These identities are checked using a SAGE program. \square

2.3 The caduceus relation

In addition to the Yang-Baxter equation, the stochastic symplectic ice also satisfies a further relation called the “caduceus relation”, which plays an important role in deriving functional equations for the partition functions in Section 2.4. Namely, we have the following

Theorem 2.2. Assume that A is stochastic $\Gamma - \Gamma$ vertex, B is stochastic $\Delta - \Delta$ vertex, C is stochastic $\Delta - \Gamma$ vertex, and D is stochastic $\Gamma - \Delta$ vertex. Also assume that the spectral parameters of the four vertices A, B, C, D are all z_i, z_j . Denote by $Z(I_1(\epsilon_1, \epsilon_2, \epsilon_3, \epsilon_4))$ the partition function of the following configuration

with fixed combination of spins $\epsilon_1, \epsilon_2, \epsilon_3, \epsilon_4$.

$$I_1(\epsilon_1, \epsilon_2, \epsilon_3, \epsilon_4) = \begin{array}{c} \text{Diagram of a 4-pointed star with boundary spins } \epsilon_1, \epsilon_2, \epsilon_3, \epsilon_4 \text{ entering and exiting at the vertices } A, B, C, D. \end{array} \quad (2.3)$$

Also denote by $Z(I_2(\epsilon_1, \epsilon_2, \epsilon_3, \epsilon_4))$ the partition function of the following configuration with fixed combination of spins $\epsilon_1, \epsilon_2, \epsilon_3, \epsilon_4$.

$$I_2(\epsilon_1, \epsilon_2, \epsilon_3, \epsilon_4) = \begin{array}{c} \text{Diagram of two separate loops, one for } \epsilon_1 \text{ and } \epsilon_2, \text{ and another for } \epsilon_3 \text{ and } \epsilon_4. \end{array} \quad (2.4)$$

Then for any fixed combination of spins $\epsilon_1, \epsilon_2, \epsilon_3, \epsilon_4$, and for both choices of cap weights given in Figures 4-5, we have

$$Z(I_1(\epsilon_1, \epsilon_2, \epsilon_3, \epsilon_4)) = \frac{(qz_i z_j - 1)(1 - (q+1)(z_i + z_j) + (q^2 + q + 1)z_i z_j)}{q(z_i + z_j - (q+1)z_i z_j)^2} Z(I_2(\epsilon_1, \epsilon_2, \epsilon_3, \epsilon_4)). \quad (2.5)$$

Proof. There are in total $2^4 = 16$ possible combinations of the boundary spins $\epsilon_1, \epsilon_2, \epsilon_3, \epsilon_4$. The identities are checked using a SAGE program. \square

2.4 Functional equations satisfied by the partition functions

In this section, we derive functional equations satisfied by the partition functions. The main result is the following

Theorem 2.3. *Let*

$$D_1(n, L, z) = \prod_{i=1}^n z_i^L \prod_{i=1}^n (1 - (q+1)z_i + qz_i z_i'^{-1}) \quad (2.6)$$

and

$$D_2(n, L, z) = \prod_{i=1}^n z_i^L. \quad (2.7)$$

Then $\frac{Z(\mathcal{S}_{n,L,\lambda,z})}{D_1(n,L,z)}$ and $\frac{Z(\mathcal{T}_{n,L,\lambda,z})}{D_2(n,L,z)}$ are invariant under any permutation of z_1, \dots, z_n and any interchange $z_i \leftrightarrow z_i'^{-1}$.

Theorem 2.3 follows from Propositions 2.4-2.5 below. Proposition 2.4 gives a functional equation when z_1, \dots, z_n are permuted, and Proposition 2.5 gives another functional equation under the interchange $z_n \leftrightarrow \frac{1}{z_n}$. Note that $\frac{1}{z_i} + z_i' = q + 1$ for every $1 \leq i \leq n$.

Proposition 2.4. *The partition functions of the two types of stochastic symplectic ice, namely, $Z(\mathcal{S}_{n,L,\lambda,z})$ and $Z(\mathcal{T}_{n,L,\lambda,z})$, are both invariant under any permutation of z_1, \dots, z_n .*

Proposition 2.5. Let $s_n z := (z_1, \dots, z_{n-1}, \frac{1}{z_n})$. Then we have

$$Z(\mathcal{S}_{n,L,\lambda,s_n z}) = \left(\frac{1}{z_n z'_n}\right)^L \frac{1 - (q+1)z_n'^{-1} + qz_n z_n'^{-1}}{1 - (q+1)z_n + qz_n z_n'^{-1}} Z(\mathcal{S}_{n,L,\lambda,z}), \quad (2.8)$$

$$Z(\mathcal{T}_{n,L,\lambda,s_n z}) = \left(\frac{1}{z_n z'_n}\right)^L Z(\mathcal{T}_{n,L,\lambda,z}). \quad (2.9)$$

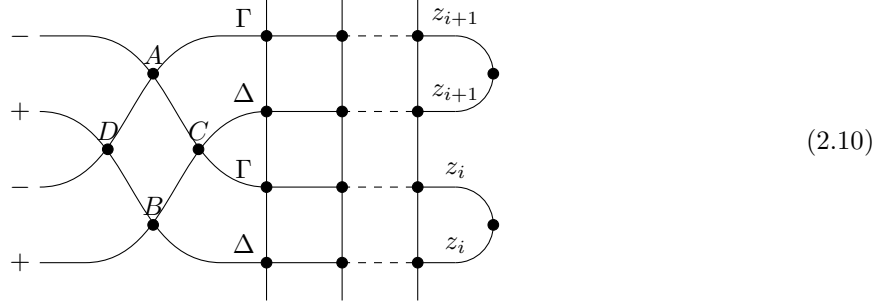
The rest of this section is devoted to the proof of Propositions 2.4-2.5. The proof of Proposition 2.4 is based on the Yang-Baxter equation and the caduceus relation. The proof of Proposition 2.5 is based on the Yang-Baxter equation and another relation called the “fish relation” (see Proposition 2.7 below).

2.4.1 Proof of Proposition 2.4

Based on Theorem 2.1 and Theorem 2.2, we give the proof of Proposition 2.4 as follows.

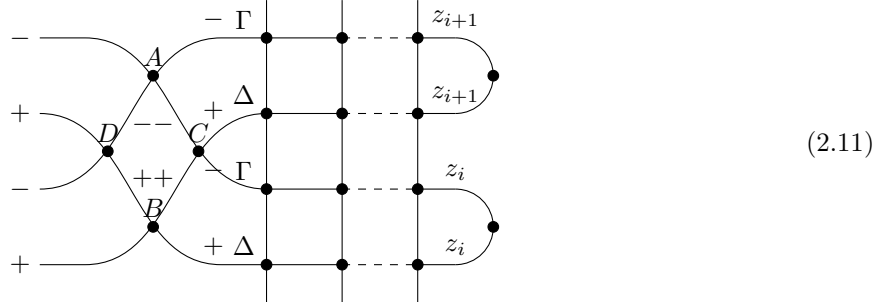
Proof of Proposition 2.4. We note that the symmetric group S_n is generated by adjacent transpositions $(i, i+1)$ for $1 \leq i \leq n-1$. Therefore it suffices to verify the invariance of the partition functions under the transposition of z_i and z_{i+1} . We show the details below for $Z(\mathcal{S}_{n,L,\lambda,z})$. The argument for $Z(\mathcal{T}_{n,L,\lambda,z})$ is essentially the same.

We attach a braid to the left boundary of the rows $2i-1, 2i, 2i+1, 2i+2$ of $\mathcal{S}_{n,L,\lambda,z}$, and obtain the following



where we have omitted the other rows of $\mathcal{S}_{n,L,\lambda,z}$. We denote by $Z(J_1)$ the partition function of this new ice model.

Note that the only admissible configuration of the braid is given as follows:



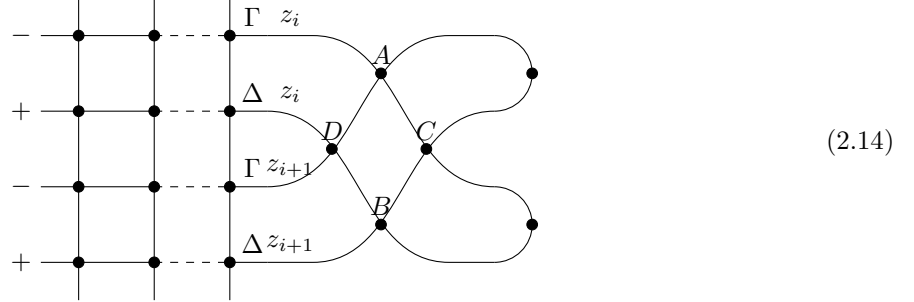
Therefore $Z(J_1)$ is the product of the partition function of the braid and $Z(\mathcal{S}_{n,L,\lambda,z})$. Let

$$L(z, q, i) = \frac{(qz_i z_{i+1} - 1)(1 - (q+1)(z_i + z_{i+1}) + (q^2 + q + 1)z_i z_{i+1})}{q(z_i + z_{i+1} - (q+1)z_i z_{i+1})^2}. \quad (2.12)$$

By computation, we obtain that

$$Z(J_1) = L(z, q, i) Z(\mathcal{S}_{n,L,\lambda,z}). \quad (2.13)$$

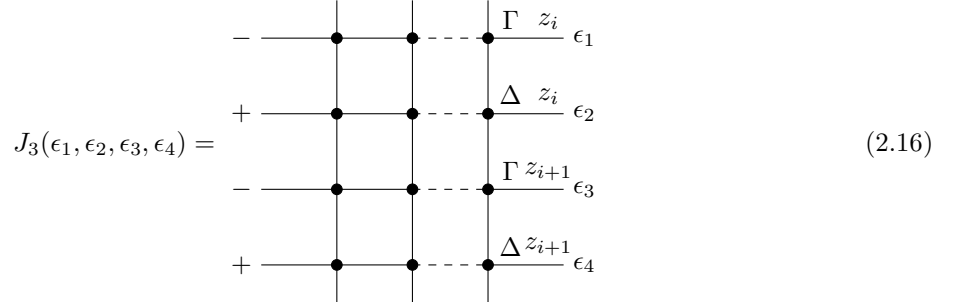
Now using the four sets of Yang-Baxter equations (Theorem 2.1), we can move the four vertices (in the order of C, A, B, D) of the braid to the right without changing the partition function. Namely, if we denote by $Z(J_2)$ the partition function of the following



then we have that

$$Z(J_1) = Z(J_2) \quad (2.15)$$

Let $J_3(\epsilon_1, \epsilon_2, \epsilon_3, \epsilon_4)$ be given as follows, and recall the definition of $I_1(\epsilon_1, \epsilon_2, \epsilon_3, \epsilon_4)$ and $I_2(\epsilon_1, \epsilon_2, \epsilon_3, \epsilon_4)$ from the statement of Theorem 2.2 (taking the spectral parameters to be z_{i+1}, z_i).



Now note that by Theorem 2.2,

$$\begin{aligned} Z(J_2) &= \sum_{\epsilon_1, \epsilon_2, \epsilon_3, \epsilon_4 \in \{-, +\}} Z(I_1(\epsilon_1, \epsilon_2, \epsilon_3, \epsilon_4)) Z(J_3(\epsilon_1, \epsilon_2, \epsilon_3, \epsilon_4)) \\ &= L(z, q, i) \sum_{\epsilon_1, \epsilon_2, \epsilon_3, \epsilon_4 \in \{-, +\}} Z(I_2(\epsilon_1, \epsilon_2, \epsilon_3, \epsilon_4)) Z(J_3(\epsilon_1, \epsilon_2, \epsilon_3, \epsilon_4)) \\ &= L(z, q, i) Z(\mathcal{S}_{n, L, \lambda, s_i z}), \end{aligned} \quad (2.17)$$

where $s_i z$ is the vector obtained by interchanging z_i, z_{i+1} from z .

By combining (2.13), (2.15), (2.17) we obtain that

$$Z(\mathcal{S}_{n, L, \lambda, z}) = Z(\mathcal{S}_{n, L, \lambda, s_i z}), \quad (2.18)$$

which finishes the proof. □

2.4.2 Proof of Proposition 2.5

Before the proof of Proposition 2.5, we make the following observation. As all the boundary edges on the top carry the + spin, we conclude that only the three states in Figure 10 are involved in the 2nth row. Now we simultaneously change the sign of the spins in the 2nth row (interchanging - and + spins), change the Boltzmann weights of the vertices in the 2nth row to those in Figure 11, and change the Boltzmann weights for the cap connecting the last two rows to those in Figure 12 or 13 (depending on the type of the stochastic

symplectic ice). For each admissible state, the Boltzmann weight of each vertex in the $2n$ th row is now scaled by a factor of $\frac{1}{qz_n}$. Therefore the partition functions of the new system, denoted by $Z(\mathcal{S}'_{n,L,\lambda,z})$ and $Z(\mathcal{T}'_{n,L,\lambda,z})$ respectively, satisfy the following

$$Z(\mathcal{S}'_{n,L,\lambda,z}) = \frac{1}{(qz_n)^L} Z(\mathcal{S}_{n,L,\lambda,z}), \quad (2.19)$$

$$Z(\mathcal{T}'_{n,L,\lambda,z}) = \frac{1}{(qz_n)^L} Z(\mathcal{T}_{n,L,\lambda,z}). \quad (2.20)$$

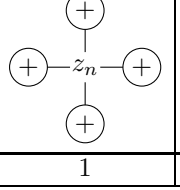
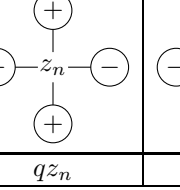
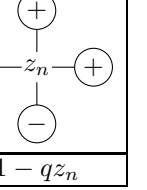
		
1	qz_n	$1 - qz_n$

Figure 10: Weights involved in the $2n$ th row

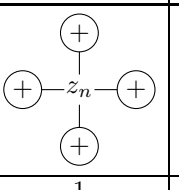
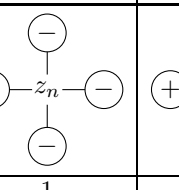
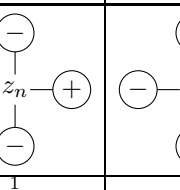
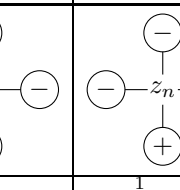
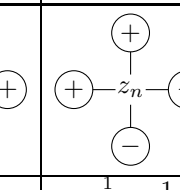
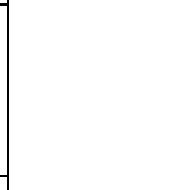
a_1	a_2	b_1	b_2	d_1	d_2
					
1	1	$\frac{1}{z_n}$	$\frac{1}{qz_n}$	$\frac{1}{z_n} - 1$	$\frac{1}{qz_n} - 1$

Figure 11: New Boltzmann weights for the $2n$ th row

New cap		
Boltzmann weight	1	1

Figure 12: New Boltzmann weights for the cap connecting the last two rows: reflecting stochastic symplectic ice

The following lemma gives a new set of Yang-Baxter equations, which will be used in the proof of Proposition 2.5.

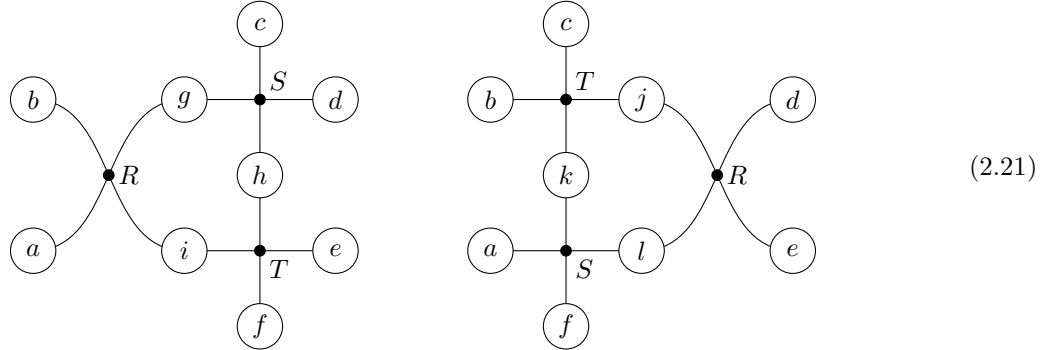
Lemma 2.6. *Assume that $t_1, t_2 \in \mathbb{C}$. Also assume that the Boltzmann weights of S are given by Figure 14, the Boltzmann weights of T are given by Figure 15, and the Boltzmann weights of R are given by Figure 16. Then the partition functions of the following two configurations are equal for any fixed combination of spins a, b, c, d, e, f .*

New cap		
Boltzmann weight	1	1

Figure 13: New Boltzmann weights for the cap connecting the last two rows: absorbing-and-emitting stochastic symplectic ice

a_1	a_2	b_1	b_2	d_1	d_2
1	1	qt_1	t_1	$qt_1 - 1$	$t_1 - 1$

Figure 14: Boltzmann weights for S : Lemma 2.6



Proof. There are $2^6 = 64$ possible combinations of boundary spins. We have checked the identities using a SAGE program. \square

Now consider the R-matrix with Boltzmann weights given by Figure 17. It is obtained by taking $t_1 = \frac{1}{qz_n}$ and $t_2 = \frac{1}{q}z'_n$ in the Boltzmann weights from Figure 16. The following theorem gives the “fish relation” satisfied by the new R-matrix and the new cap.

Proposition 2.7. *Suppose the Boltzmann weights of R in the following is given by Figure 17. Denote by $Z(I_3(\epsilon_1, \epsilon_2))$ the partition function of the following system.*

$$I_3(\epsilon_1, \epsilon_2) = \begin{array}{c} \epsilon_1 \\ \epsilon_2 \end{array} \xrightarrow{R} \text{Diagram of a fish-shaped R-matrix with boundary spins } \epsilon_1 \text{ and } \epsilon_2 \quad (2.22)$$

Also denote by $Z(I_4(\epsilon_1, \epsilon_2))$ the partition function of the following system.

$$I_4(\epsilon_1, \epsilon_2) = \begin{array}{c} \epsilon_1 \\ \epsilon_2 \end{array} \xrightarrow{R} \text{Diagram of a fish-shaped R-matrix with boundary spins } \epsilon_1 \text{ and } \epsilon_2 \quad (2.23)$$

a_1	a_2	b_1	b_2	d_1	d_2
1	1	qt_2	t_2	$1 - qt_2$	$1 - t_2$

Figure 15: Boltzmann weights for T : Lemma 2.6

a_1	a_2	b_1	b_2	c_1	c_2
1	1	$\frac{t_2 - t_1}{1 - (q+1)t_1 + qt_1 t_2}$	$\frac{q(t_2 - t_1)}{1 - (q+1)t_1 + qt_1 t_2}$	$-\frac{(1-t_2)(1-qt_1)}{1 - (q+1)t_1 + qt_1 t_2}$	$-\frac{(1-t_1)(1-qt_2)}{1 - (q+1)t_1 + qt_1 t_2}$

Figure 16: Boltzmann weights for R : Lemma 2.6

Then for reflecting stochastic symplectic ice (i.e. the Boltzmann weights for the new cap are given by Figure 12), we have

$$Z(I_3(\epsilon_1, \epsilon_2)) = -\frac{1 - (q+1)z_n + qz_n z_n'^{-1}}{1 - (q+1)z_n'^{-1} + qz_n z_n'^{-1}} Z(I_4(\epsilon_1, \epsilon_2)); \quad (2.24)$$

for absorbing-and-emitting stochastic symplectic ice (i.e. the Boltzmann weights for the new cap are given by Figure 13), we have

$$Z(I_3(\epsilon_1, \epsilon_2)) = Z(I_4(\epsilon_1, \epsilon_2)). \quad (2.25)$$

Proof. We denote by $a_1, a_2, b_1, b_2, c_1, c_2$ the Boltzmann weights for the R-matrix.

First consider reflecting stochastic symplectic ice. In this case $Z(I_3(+, +)) = Z(I_3(-, -)) = Z(I_4(+, +)) = Z(I_4(-, -)) = 0$. Moreover,

$$Z(I_3(+, -)) = c_1 + b_2 = -\frac{1 - (q+1)z_n + qz_n z_n'^{-1}}{1 - (q+1)z_n'^{-1} + qz_n z_n'^{-1}} Z(I_4(+, -)), \quad (2.26)$$

$$Z(I_3(-, +)) = c_2 + b_1 = -\frac{1 - (q+1)z_n + qz_n z_n'^{-1}}{1 - (q+1)z_n'^{-1} + qz_n z_n'^{-1}} Z(I_4(-, +)). \quad (2.27)$$

Now consider absorbing-and-emitting stochastic symplectic ice. In this case $Z(I_3(+, -)) = Z(I_3(-, +)) = Z(I_4(+, -)) = Z(I_4(-, +)) = 0$. Moreover,

$$Z(I_3(+, +)) = a_1 = Z(I_4(+, +)), \quad (2.28)$$

$$Z(I_3(-, -)) = a_2 = Z(I_4(-, -)). \quad (2.29)$$

□

We finish the proof of Proposition 2.5 as follows.

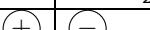
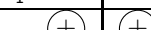
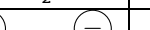
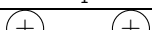
a_1	a_2	b_1	b_2	c_1	c_2
					
1	1	$\frac{z_n z'_n - 1}{qz_n + z'_n - (q+1)}$	$\frac{q(z_n z'_n - 1)}{qz_n + z'_n - (q+1)}$	$-\frac{(z_n - 1)(q - z'_n)}{qz_n + z'_n - (q+1)}$	$-\frac{(qz_n - 1)(1 - z'_n)}{qz_n + z'_n - (q+1)}$

Figure 17: The R-matrix used in the proof of Proposition 2.5

Proof of Proposition 2.5. For ease of notations, we denote by $V(a_1, a_2, b_1, b_2, c_1, c_2, d_1, d_2)$ a vertex with Boltzmann weights given by $a_1, a_2, b_1, b_2, c_1, c_2, d_1, d_2$.

Now we attach the R-matrix given by Figure 17 to the left boundary of the last two rows of the changed system:

$$\begin{array}{c}
\text{Diagram showing a crossing of two lines labeled } R \text{ and } z_n. \text{ The left side has two '+' signs. The right side shows two vertical lines with dots at the top and bottom, and a horizontal line connecting them. A dashed line goes from the top dot to the right, and a solid line goes from the bottom dot to the right. The top dashed line has a loop that goes up, then right, then down, then right again. The bottom solid line has a loop that goes up, then right, then down, then right again. The top dashed line is labeled } V(1, 1, \frac{1}{z_n}, \frac{1}{qz_n}, 0, 0, \frac{1}{z_n} - 1, \frac{1}{qz_n} - 1) \text{ and the bottom solid line is labeled } V(1, 1, z'_n, \frac{1}{q}z'_n, 0, 0, 1 - z'_n, 1 - \frac{1}{q}z'_n) \text{.}
\end{array} \tag{2.30}$$

Note that the only admissible configuration of the R-matrix is given by

$$\begin{array}{c}
\text{Diagram:} \\
\begin{array}{c}
\text{A directed graph with 8 nodes arranged in two rows of four. The top row has nodes } R, \bullet, \bullet, \bullet \text{ and the bottom row has nodes } \bullet, \bullet, \bullet, \bullet. \\
\text{Arrows: } R \rightarrow \bullet, \bullet \rightarrow \bullet. \\
\text{Labels: } + \text{ is at the leftmost node } R, + \text{ is at the bottom-left node, } + \text{ is at the bottom-middle node, } + \text{ is at the bottom-right node, } V(1, 1, \frac{1}{z_n}, \frac{1}{qz_n}, 0, 0, \frac{1}{z_n} - 1, \frac{1}{qz_n} - 1) \text{ is at the top-right node, } V(1, 1, z'_n, \frac{1}{q}z'_n, 0, 0, 1 - z'_n, 1 - \frac{1}{q}z'_n) \text{ is at the bottom-right node.}
\end{array}
\end{array} \tag{2.31}$$

Therefore, the partition function of the above system is equal to $Z(\mathcal{S}'_{n,L,\lambda,z})$ or $Z(\mathcal{T}'_{n,L,\lambda,z})$ according to the type of the stochastic symplectic ice.

By Lemma 2.6, the R-matrix can be pushed to the right without changing the partition function. That is, the partition function of the above system is equal to the partition function of the following

$$\begin{array}{c}
+ \quad \bullet \quad + \\
+ \quad \bullet \quad + \\
\hline
V(1, 1, z'_n, \frac{1}{q}z'_n, 0, 0, 1 - z'_n, 1 - \frac{1}{q}z'_n) \\
V(1, 1, \frac{1}{z_n}, \frac{1}{qz_n}, 0, 0, \frac{1}{z_n} - 1, \frac{1}{qz_n} - 1)
\end{array} \quad (2.32)$$

Consider the reflecting stochastic symplectic ice. By Proposition 2.7, the above partition function is equal to $-\frac{1-(q+1)z_n+qz_nz_{n-1}^{q-1}}{1-(q+1)z_n^{q-1}+qz_nz_{n-1}^{q-1}}$ times the partition function of the following system (denoted by Z_1)

We note again that the top boundary edges of the system all carry + spin. We change the sign of the spins of the 2nth row again (interchanging + and -), and also change the Boltzmann weights of the 2nth

row as in the following configuration. The Boltzmann weights for the cap connecting the last two rows are changed back to the original one given in Figure 4. We denote the partition function of the following system by Z_2 .

Similar to the previous argument, we conclude that

$$Z_2 = \left(\frac{q}{z'_n}\right)^L Z_1. \quad (2.35)$$

Now note that the total number of c_1, c_2, d_1, d_2 patterns in the last two rows is an odd number (as can be seen by interpreting spins as paths and considering all possibilities). Hence Z_2 is equal to -1 times the partition function of the following configuration, which is $Z(\mathcal{S}_{n,L,\lambda,s_nz})$.

Therefore we conclude that

$$Z(\mathcal{S}_{n,L,\lambda,s_nz}) = \left(\frac{1}{z_n z_n'}\right)^L \frac{1 - (q+1)z_n'^{-1} + qz_n z_n'^{-1}}{1 - (q+1)z_n + qz_n z_n'^{-1}} Z(\mathcal{S}_{n,L,\lambda,z}). \quad (2.37)$$

The conclusion for $Z(\mathcal{T}_{n,L,\lambda,s_n}z)$ can be obtained similarly, noting that the number of c_1, c_2, d_1, d_2 patterns in the last two rows is an even number for this case.

3 Colored stochastic symplectic ice

In this section, we introduce a colored version of the stochastic symplectic ice model. For each edge of the rectangular lattice, instead of assigning either a + or - spin, we now associate either + or one of $2n$ colors to it. The $2n$ colors are labeled by $[\pm n] = \{\bar{n}, \dots, \bar{1}, 1, \dots, n\}$.

The colored model is closely related to Cartan type C: part of the boundary conditions are specified by two elements of the hyperoctahedral group, the Weyl group of type C; the recursive relations for the partition function, upon a change of variables, are related to Demazure-Lusztig operators of type C.

We start by introducing the colored model in Section 3.1. Then we introduce the R-matrix and prove the Yang-Baxter equation in Section 3.2. In Section 3.3, we compute the partition function when $\sigma(i) = \overline{\tau(i)}$ for every $1 \leq i \leq n$. Then we present a new relation, the reflection equation, in Section 3.4. By combining the Yang-Baxter equation and the reflection equation, we derive the recursive relations for the partition function in Section 3.5. The recursive relations are further related to Demazure-Lusztig operators of type C in Section 3.6.

We briefly introduce the hyperoctahedral group, denoted by B_n , here. The hyperoctahedral group has the following presentation

$$B_n = \langle s_1, \dots, s_n | s_i^2 = 1, 1 \leq i \leq n; (s_i s_{i+1})^3 = 1, 1 \leq i \leq n-2; (s_{n-1} s_n)^4 = 1; (s_i s_j)^2 = 1, 1 \leq i < j \leq n, |i-j| > 1 \rangle.$$

The group B_n is the Weyl group for the root system of type C_n . Elements of B_n can be viewed as permutations σ of $[\pm n]$ such that $\sigma(-i) = -\sigma(i)$ for every $1 \leq i \leq n$.

We make the convention that elements of B_n are multiplied from right to left, and that $\bar{i} = i$ for each $1 \leq i \leq n$. Thus for each $i \in [\pm n]$ and $\sigma, \tau \in B_n$, we have $\sigma\tau(i) = \sigma(\tau(i))$. Note that s_i is the transposition $(i, i+1)$ for each $1 \leq i \leq n-1$, and that $s_n(i) = i$ for $1 \leq i \leq n-1$ and $s_n(n) = \bar{n}$.

3.1 The colored model

We introduce the colored version of the stochastic symplectic ice in this section. The main difference from the uncolored model is that now every edge of the lattice can either take + or one of the $2n$ colors labeled by $[\pm n]$.

We denote the colors by $c_{\bar{n}}, \dots, c_n$. Hereafter we refer to c_i and $c_{\bar{i}}$ as mutually opposite colors for every $1 \leq i \leq n$. For convenience of notations, we also let $c_0 := +$. We take the following order on the colors (including c_0):

$$\bar{n} < \dots < \bar{1} < 0 < 1 < \dots n. \quad (3.1)$$

In the colored model, there are also two types of vertices. They are termed ‘‘colored stochastic Γ vertex’’ and ‘‘colored stochastic Δ vertex’’. The model depends on n spectral parameters z_1, \dots, z_n and a deformation parameter q . Again we take

$$z'_i = q + 1 - \frac{1}{z_i}.$$

The Boltzmann weights for the two types of vertices are listed in Figures 18-19.

a_1/a_2	a_1/a_2	b_1	b_2	c_1	c_2
1	1	z_i	qz_i	$1 - qz_i$	$1 - z_i$

Figure 18: Boltzmann weights for colored stochastic Γ vertex with spectral parameter z_i , where $\alpha < \beta$

a_1/a_2	a_1/a_2	b_1	b_2	d_1	d_2
1	1	z'_i	$\frac{1}{q}z'_i$	$1 - z'_i$	$1 - \frac{1}{q}z'_i$

Figure 19: Boltzmann weights for colored stochastic Δ vertex with spectral parameter z_i , where $\alpha < \beta$ and $z'_i = q + 1 - \frac{1}{z_i}$

The colored model consists of a rectangular lattice with $2n$ rows and L columns. The rows are numbered $1, 2, \dots, 2n$ from bottom to top, and the columns are numbered $1, 2, \dots, L$ from right to left. Every odd-numbered row is a row of colored stochastic Δ vertex, and every even-numbered row is a row of colored stochastic Γ vertex. The spectral parameter for the i th row of colored stochastic Γ vertices and the i th row of the colored stochastic Δ vertices is z_i .

The model also depends on a partition $\lambda = (\lambda_1, \dots, \lambda_n) \in \mathbb{Z}^n$ (with $\lambda_1 \geq \dots \geq \lambda_n$) and two elements $\sigma, \tau \in B_n$, where B_n is the hyperoctahedral group as introduced previously. We assume that $L \geq \lambda_1 + n$. The assignment of boundary conditions is given as follows: on the left column, we assign color $c_{\sigma(i)}$ to the i th row of colored stochastic Γ vertex, and $+$ to each row of colored stochastic Δ vertex; on the top, we assign $+$ to each boundary edge; on the bottom, we assign color $c_{\tau(i)}$ to each column labeled $\lambda_i + n + 1 - i$ for $1 \leq i \leq n$, and assign $+$ to the other columns. On the right, the i th row of colored stochastic Γ vertex and the i th row of colored stochastic Δ vertex are connected with a cap. The Boltzmann weights for the caps are given in Figure 20.

Cap			
Boltzmann weight	1	1	1

Figure 20: Boltzmann weights of the caps for colored stochastic symplectic ice: where $\alpha \in \{1, 2, \dots, n\}$

Hereafter we denote by $\mathcal{S}_{n,L,\lambda,\sigma,\tau,z}$ the collection of admissible configurations with the above specified data. We also denote by $Z(\mathcal{S}_{n,L,\lambda,\sigma,\tau,z})$ the corresponding partition function.

We note that the Boltzmann weights for both types of vertices and the caps are also stochastic, as in the uncolored case. When z satisfies the condition (2.1), a probabilistic interpretation for each vertex can similarly be obtained.

We also note that the colored model can be interpreted as an interacting particle system as in the uncolored case if condition (2.1) is satisfied. The interpretation is similar to the uncolored case, except that now each particle carries a color, and that the updating rule for the particle depends on its color.

The detailed rule is as follows. When t is even, the particles are ordered from left to right. There is a new particle entering from the left boundary with color $c_{\sigma(n-\frac{t}{2})}$ (we call it 0th particle), which jumps to the right with geometric jump size (with parameter $qz_{n-\frac{t}{2}}$ if $\sigma(n-\frac{t}{2}) > 0$, or $z_{n-\frac{t}{2}}$ otherwise) unless it hits the 1st particle; if the particle hits the 1st particle, the updating rule will be described later. Starting from $l = 1$, if the l th particle wasn't hit by any particle on its left, we flip a coin with head probability $z_{n-\frac{t}{2}}$ (if the color of the particle is c_α with $\alpha > 0$) or $qz_{n-\frac{t}{2}}$ (if $\alpha < 0$) to determine whether it will stay at its current position; if the coin comes up tail, then the particle jumps to the right with geometric jump size (with parameter $qz_{n-\frac{t}{2}}$ if $\alpha > 0$, or $z_{n-\frac{t}{2}}$ if $\alpha < 0$) unless it hits the $(l+1)$ th particle; if the particle hits the $(l+1)$ th particle, the updating rule will be described later. If the l th particle was hit by the $(l-1)$ th particle, either the $(l-1)$ th or the l th particle (depending on the updating rule as will be described later) jumps to the right by 1 and the following move is the same as the previous case except for the first step determining whether it will stay at the current position. Then the $(l+1)$ th particle begins to move. If the rightmost particle moves beyond the first column (meaning that it hits the cap), it is reflected by the cap (meaning that it will start to move leftward from the first column at time $t+1$), and its color c_α is changed to $c_{\bar{\alpha}}$.

When t is odd, the particles are ordered from right to left. If there is a particle reflected from the cap (we call it 0th particle), it jumps to the left with geometric jump size (with parameter $\frac{1}{q}z'_{n-\frac{t-1}{2}}$ if the color of the particle is c_α with $\alpha > 0$, or $z'_{n-\frac{t-1}{2}}$ otherwise) unless it hits the 1st particle; if the particle hits the 1st particle, the updating rule will be described later. Starting from $l = 1$, if the l th particle wasn't hit by any particle on its right, we flip a coin with head probability $z'_{n-\frac{t-1}{2}}$ (if the color of the particle is c_α with $\alpha > 0$) or $\frac{1}{q}z'_{n-\frac{t-1}{2}}$ (if $\alpha < 0$) to determine whether it will stay at its current position; if the coin comes up tail, then the particle jumps to the left with geometric jump size (with parameter $\frac{1}{q}z'_{n-\frac{t-1}{2}}$ if $\alpha > 0$, or $z'_{n-\frac{t-1}{2}}$ if $\alpha < 0$) unless it hits the $(l+1)$ th particle; if the particle hits the $(l+1)$ th particle, the updating rule will be described later. If the l th particle was hit by the $(l-1)$ th particle, either the $(l-1)$ th or the l th particle (depending on the updating rule as will be described later) jumps to the left by 1 and the following

move is the same as the previous case except for the first step determining whether it will stay at the current position. Then the $(l+1)$ th particle begins to move.

Now we describe the updating rule for the case when a particle hits another. When the time t is even, consider the situation when a particle of color c_α hits another particle of color c_β from the left. If $\alpha < \beta$, with probability $z_{n-\frac{t}{2}}$ the two particles are swapped, with the particle of color c_β staying at the original position and the other particle continuing to move; with probability $1 - z_{n-\frac{t}{2}}$, the particle of color c_α stays at the current position and the other particle starts to move. If $\alpha > \beta$, with probability $qz_{n-\frac{t}{2}}$ the two particles are swapped, with the particle of color c_β staying at the original position and the other particle continuing to move; with probability $1 - qz_{n-\frac{t}{2}}$, the particle of color c_α stays at the current position and the other particle starts to move.

When the time t is odd, we also consider the situation when a particle of color c_α hits another particle of color c_β from the right. If $\alpha < \beta$, with probability $z'_{n-\frac{t-1}{2}}$ the two particles are swapped, with the particle of color c_β staying at the original position and the other particle continuing to move; with probability $1 - z'_{n-\frac{t-1}{2}}$, the particle of color c_α stays at the current position and the other particle starts to move. If $\alpha > \beta$, with probability $\frac{1}{q}z'_{n-\frac{t-1}{2}}$ the two particles are swapped, with the particle of color c_β staying at the original position and the other particle continuing to move; with probability $1 - \frac{1}{q}z'_{n-\frac{t-1}{2}}$, the particle of color c_α stays at the current position and the other particle starts to move.

Under this probabilistic interpretation, the partition function $Z(\mathcal{S}_{n,L,\lambda,\sigma,\tau,z})$ represents the probability that (with the entering order of particle colors specified by σ) the particle configuration at time $t = 2n$ is given by μ and τ , with μ specifying the particle locations and τ specifying the particle colors.

3.2 The R-matrix and the Yang-Baxter equation

For the colored stochastic symplectic ice, we find three sets of Yang-Baxter equations. The corresponding R-matrices are termed “colored stochastic $\Gamma - \Gamma$ vertex”, “colored stochastic $\Delta - \Gamma$ vertex” and “colored stochastic $\Delta - \Delta$ vertex”. In Section 3.5 we will show that, when combined with the reflection equation, these three sets of Yang-Baxter equations are enough for us to derive the recursive relations for the partition functions.

Throughout the paper we denote the Boltzmann weights of an R-matrix of type XY and spectral parameters z_i, z_j as shown in Figure 21 by $R_{XY}(c_\alpha, c_\beta, c_\gamma, c_\delta; z_i, z_j)$, where $(X, Y) \in \{(\Gamma, \Gamma), (\Delta, \Delta), (\Delta, \Gamma)\}$ and $\alpha, \beta, \gamma, \delta \in \{\bar{n}, \dots, \bar{1}, 0, 1, \dots, n\}$. The Boltzmann weights for the three types of R-matrices are given in Figures 22-24.

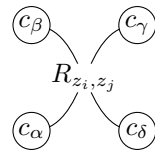


Figure 21: R-matrix

The following theorem gives the three sets of Yang-Baxter equations for the colored stochastic symplectic ice.

Theorem 3.1. *For any $(X, Y) \in \{(\Delta, \Gamma), (\Gamma, \Gamma), (\Delta, \Delta)\}$ the following holds. Assume that S is colored stochastic X vertex with spectral parameter z_i , T is colored stochastic Y vertex with spectral parameter z_j , and R is colored stochastic $X - Y$ vertex with spectral parameters z_i, z_j . Then the partition functions of the*

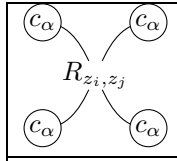
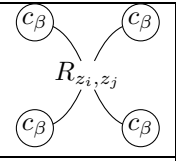
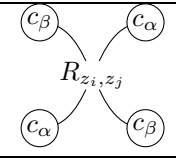
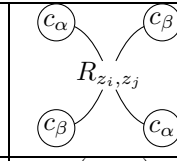
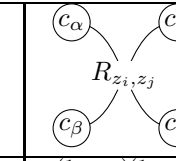
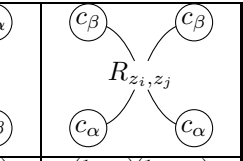
					
1	1	$\frac{z_i - z_j}{1 - (q+1)z_j + qz_i z_j}$	$\frac{q(z_i - z_j)}{1 - (q+1)z_j + qz_i z_j}$	$\frac{(1 - qz_i)(1 - z_j)}{1 - (q+1)z_j + qz_i z_j}$	$\frac{(1 - z_i)(1 - qz_j)}{1 - (q+1)z_j + qz_i z_j}$

Figure 22: Boltzmann weights for colored stochastic $\Gamma - \Gamma$ vertex with spectral parameters z_i and z_j : where $\alpha < \beta$

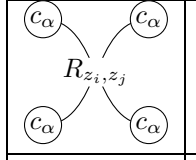
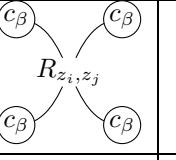
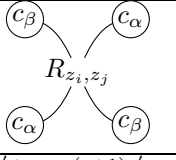
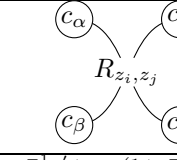
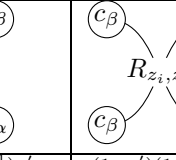
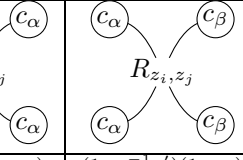
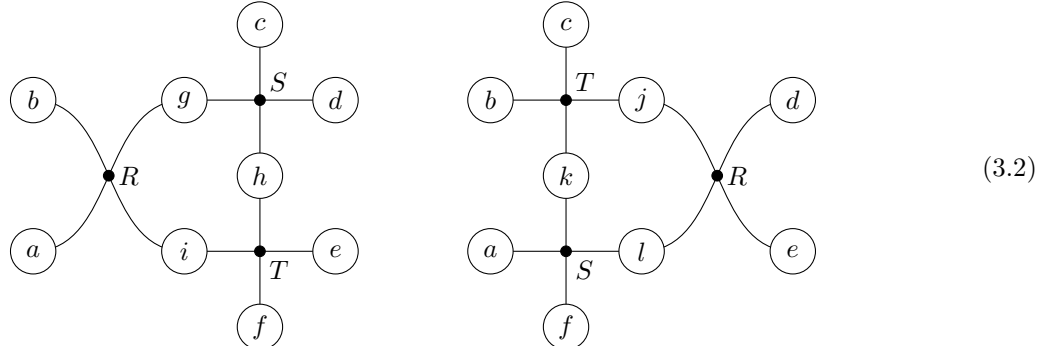
					
1	1	$\frac{z'_i + qz_j - (q+1)z'_i z_j}{1 - z'_i z_j}$	$\frac{q^{-1}z'_i + z_j - (1 + q^{-1})z'_i z_j}{1 - z'_i z_j}$	$\frac{(1 - z'_i)(1 - qz_j)}{1 - z'_i z_j}$	$\frac{(1 - q^{-1}z'_i)(1 - z_j)}{1 - z'_i z_j}$

Figure 23: Boltzmann weights for colored stochastic $\Delta - \Gamma$ vertex with spectral parameters z_i and z_j : where $\alpha < \beta$

following two configurations are equal for any fixed combination of colors $a, b, c, d, e, f \in \{c_{\bar{n}}, \dots, c_0, \dots, c_n\}$.



Proof. From conservation of colors for both colored stochastic Γ vertices and colored stochastic Δ vertices (note that the directions of input and output are different for these two types of vertices), it can be checked that at most four distinct colors (including c_0) can appear on the boundary edges in any of the two configurations, and that the color on an inner edge must be one of the colors on boundary edges (only considering admissible configurations). Moreover, the Boltzmann weight of a vertex only depends on the relative order of the colors on its adjacent four edges. Therefore it suffices to check the result for four colors, and there are at most 4^6 possible combinations of boundary colors. These identities are checked using a SAGE program. \square

3.3 Evaluation of the partition function when $\sigma(i) = \overline{\tau(i)}$

When $\sigma(i) = \overline{\tau(i)}$ for every $1 \leq i \leq n$, the partition function $Z(S_{n,L,\lambda,\sigma,\tau,z})$ has a relatively simple form, as is shown in the following theorem.

1	1	$\frac{z'_j - z'_i}{q - (q+1)z'_i + z'_i z'_j}$	$\frac{q(z'_j - z'_i)}{q - (q+1)z'_i + z'_i z'_j}$	$\frac{(1-z'_i)(q-z'_j)}{q - (q+1)z'_i + z'_i z'_j}$	$\frac{(1-z'_j)(q-z'_i)}{q - (q+1)z'_i + z'_i z'_j}$

Figure 24: Boltzmann weights for colored stochastic $\Delta - \Delta$ vertex with spectral parameters z_i and z_j : where $\alpha < \beta$

Theorem 3.2. *If σ and τ satisfy the condition that $\sigma(i) = \overline{\tau(i)}$ for every $1 \leq i \leq n$, then we have*

$$\begin{aligned} Z(\mathcal{S}_{n,L,\lambda,\sigma,\tau,z}) &= \prod_{i=1}^n z_i^L \prod_{i=1}^n \left(\frac{z'_i}{q}\right)^{\lambda_i+n-i} \prod_{i=1}^n (1 - q^{-1_{\sigma(i)<0}} z'_i) \\ &\times q^{\sum_{i=1}^n (L-n+i+\lambda_i) \mathbf{1}_{\sigma(i)>0} + \sum_{1 \leq i < j \leq n} (\mathbf{1}_{\overline{\sigma(j)} < \sigma(i)} + \mathbf{1}_{\sigma(j) < \sigma(i)})}. \end{aligned} \quad (3.3)$$

In particular, if $\sigma(i) = \overline{i}$ and $\tau(i) = i$ for every $1 \leq i \leq n$, then

$$Z(\mathcal{S}_{n,L,\lambda,\sigma,\tau,z}) = \prod_{i=1}^n z_i^L \prod_{i=1}^n \left(\frac{z'_i}{q}\right)^{\lambda_i+n-i} \prod_{i=1}^n \left(1 - \frac{z'_i}{q}\right) q^{\frac{n(n-1)}{2}}. \quad (3.4)$$

Proof. We use the colored path interpretation. An illustration of the proof is shown in Figure 25, where we assume that $c_1 = B$, $c_2 = R$, $c_{\overline{1}} = \overline{B}$, $c_{\overline{2}} = \overline{R}$. We say that c_i and $c_{\overline{i}}$ are of the same color type for $1 \leq i \leq n$ (and c_0 itself forms a color type). The collection of the particles with the same color type are viewed as a colored path. Each path enters from the left boundary, moves rightward or downward on each row of colored stochastic Γ vertex, and moves leftward or downward on each row of colored stochastic Δ vertex. When the path enters the cap on a row of colored stochastic Γ vertex, it will bend through the cap, change the color to its opposite, and restart on the right-most vertex of the row of colored stochastic Δ vertex just below the previous row. Finally, the colored path leaves the rectangular lattice at the bottom boundary.

Consider the colored path entering from the 2nd row, which has color $c_{\sigma(1)}$. In order for the path to leave the domain with an opposite color (which is required by the boundary condition, as $\tau(1) = \overline{\sigma(1)}$), it has to move rightward until it goes through the cap. Then the path changes its color to $c_{\tau(1)}$ and leaves the domain at the column labeled as $\lambda_1 + n$.

Now consider the colored path entering from the 4th row, which has color $c_{\sigma(2)}$. In order for the path to leave the domain with an opposite color, it has to move rightward until it goes through the cap (as the cap connecting the first two rows has already been taken by the colored path entering from the 2nd row). Then note that $\lambda_1 + n > \lambda_2 + n - 1$. In order for the path to leave at the column labeled $\lambda_2 + n - 1$, it has to move leftward after passing the cap until it reaches the column labeled $\lambda_2 + n - 1$. After that it moves downward until it leaves the domain.

The rest of the colored paths can be analyzed similarly. The colored path entering from the $(2i)$ th row first moves rightward until it goes through the cap (and changes the color to its opposite), then it moves leftward until it reaches the column labeled $\lambda_i + n + 1 - i$, and finally it moves downward until it leaves the domain.

The above analysis shows that there is only one admissible state. Computing the Boltzmann weight of this state finishes the proof. \square

3.4 The reflection equation

Due to the lack of the R-matrix and the Yang-Baxter equation for the colored stochastic Γ vertex and the colored stochastic Δ vertex, we cannot use the caduceus relation as in the uncolored model. However,

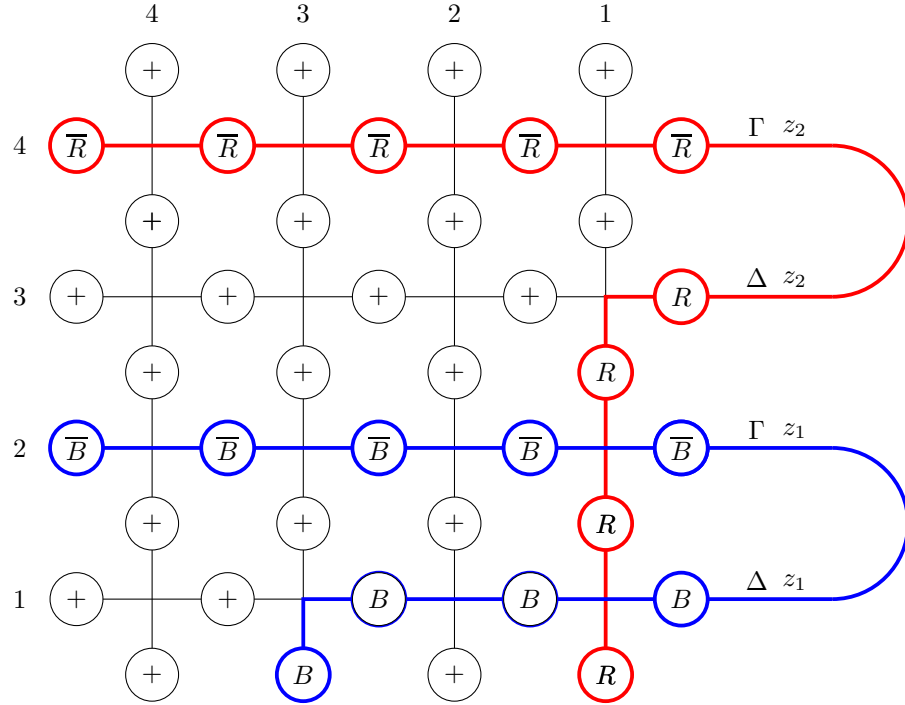
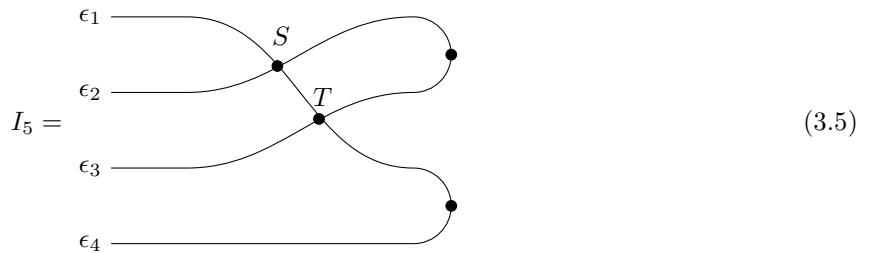


Figure 25: Illustration of the proof of Theorem 3.2

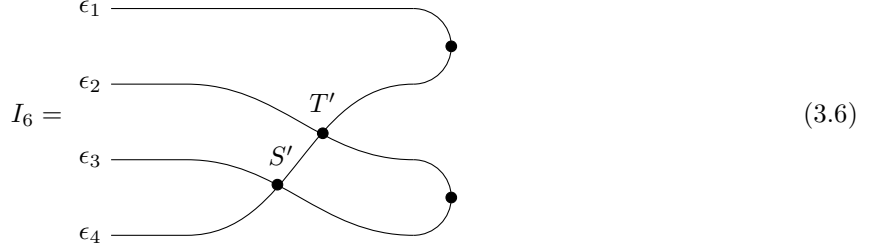
another set of relations, the reflection equation, provides an alternative way to derive recursive relations of the partition function. The following theorem gives the reflection equation.

Theorem 3.3. Assume that S is colored stochastic $\Gamma - \Gamma$ vertex of spectral parameters z_i, z_j , T is colored stochastic $\Delta - \Gamma$ vertex of spectral parameters z_i, z_j , S' is colored stochastic $\Delta - \Delta$ vertex of spectral parameters z_j, z_i , and T' is colored stochastic $\Delta - \Gamma$ vertex of spectral parameters z_j, z_i . Denote by $Z(I_5(\epsilon_1, \epsilon_2, \epsilon_3, \epsilon_4))$ the partition function of the following configuration with fixed combination of colors $\epsilon_1, \epsilon_2, \epsilon_3, \epsilon_4 \in \{c_{\bar{n}}, \dots, c_0, \dots, c_n\}$.



Also denote by $Z(I_6(\epsilon_1, \epsilon_2, \epsilon_3, \epsilon_4))$ the partition function of the following configuration with fixed combination

of colors $\epsilon_1, \epsilon_2, \epsilon_3, \epsilon_4 \in \{c_{\bar{n}}, \dots, c_0, \dots, c_n\}$.



Then for any fixed combination of colors $\epsilon_1, \epsilon_2, \epsilon_3, \epsilon_4 \in \{c_{\bar{n}}, \dots, c_0, \dots, c_n\}$, we have

$$Z(I_5(\epsilon_1, \epsilon_2, \epsilon_3, \epsilon_4)) = Z(I_6(\epsilon_1, \epsilon_2, \epsilon_3, \epsilon_4)). \quad (3.7)$$

Proof. We say that c_α and c_β are of the same color type, if $\beta = \bar{\alpha}$ (c_0 itself forms a color type). From conservation of colors for the R-matrix and the cap weights, we can deduce that for any admissible state of I_5 or I_6 , each color type must appear for an even number of times in $\{\epsilon_1, \epsilon_2, \epsilon_3, \epsilon_4\}$, and that the color type of an inner edge must be one of the color types of $\{\epsilon_1, \epsilon_2, \epsilon_3, \epsilon_4\}$. From this we can further deduce that at most two color types can appear in $\{\epsilon_1, \epsilon_2, \epsilon_3, \epsilon_4\}$ in any admissible state of I_5 or I_6 . Moreover, we note that the Boltzmann weight for the R-matrix only depends on the relative order of colors on its four adjacent edges. Therefore it suffices to check the relation for five colors $\{c_2, c_1, c_0, c_1, c_2\}$. There are at most 5^4 combinations of $(\epsilon_1, \epsilon_2, \epsilon_3, \epsilon_4)$ for this case. These identities have been checked using a SAGE program. \square

3.5 Recursive relations of the partition function

In this section, we derive recursive relations of the partition function. The recursive relations are further related to Demazure-Lusztig operators of type C in Section 3.6. The main results are Theorems 3.4-3.5.

Theorem 3.4. Assume that $1 \leq i \leq n-1$ and $\sigma(i+1) > \sigma(i)$. Let s_i be the transposition $(i, i+1)$ in B_n , and let $s_i z$ be the vector obtained from z by interchanging z_i, z_{i+1} . Then the partition function of the colored stochastic symplectic ice satisfies the following recursive relation:

$$q^{1_{\sigma(i+1)>0} - 1_{\sigma(i)>0}} Z(\mathcal{S}_{n, L, \lambda, \sigma s_i, \tau, z}) = -A(q, z, i) Z(\mathcal{S}_{n, L, \lambda, \sigma, \tau, z}) + B(q, z, i) Z(\mathcal{S}_{n, L, \lambda, \sigma, \tau, s_i z}), \quad (3.8)$$

where

$$A(q, z, i) = \frac{(1 - z_{i+1})(1 - qz_i)}{z_{i+1} - z_i}, \quad (3.9)$$

and

$$B(q, z, i) = \frac{1 - (q+1)z_i + qz_i z_{i+1}}{z_{i+1} - z_i}. \quad (3.10)$$

Theorem 3.5. Assume that $\sigma(n) > 0$. Let s_n be the element of B_n that changes the sign of the element at the n th position, and

$$s_n z = (z_1, \dots, z_{n-1}, \frac{1}{z'_n}). \quad (3.11)$$

Then we have

$$(\frac{q}{z_n})^L Z(\mathcal{S}_{n, L, \lambda, \sigma s_n, \tau, z}) = C(q, z) z_n^{-L} Z(\mathcal{S}_{n, L, \lambda, \sigma, \tau, z}) - D(q, z) z_n'^L Z(\mathcal{S}_{n, L, \lambda, \sigma, \tau, s_n z}). \quad (3.12)$$

where

$$C(q, z) = \frac{(q - z'_n)(z_n - 1)}{q(1 - z_n z'_n)}, \quad (3.13)$$

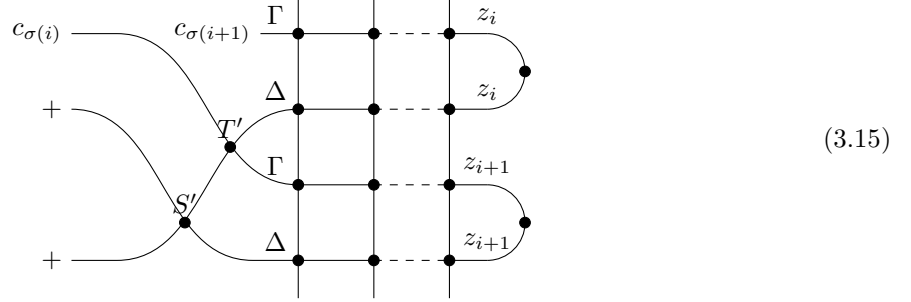
$$D(q, z) = \frac{qz_n + z'_n - (q+1)z_n z'_n}{q(1 - z_n z'_n)}. \quad (3.14)$$

The rest of this section is devoted to the proof of Theorems 3.4-3.5.

3.5.1 Proof of Theorem 3.4

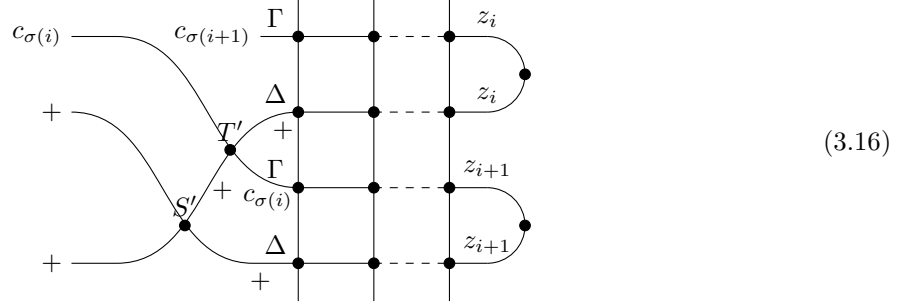
The proof of Theorem 3.4 is based on the Yang-Baxter equation (Theorem 3.1) and the reflection equation (Theorem 3.3).

Proof of Theorem 3.4. We attach two R-vertices to the left of $\mathcal{S}_{n,L,\lambda,\sigma,\tau,s_i z}$, as shown in the following



where we omit the other rows of $\mathcal{S}_{n,L,\lambda,\sigma,\tau,s_i z}$, S' is colored stochastic $\Delta - \Delta$ vertex of spectral parameters z_i, z_{i+1} , and T' is colored stochastic $\Delta - \Gamma$ R-vertex of spectral parameters z_i, z_{i+1} . We denote by Z_1 the partition function of this new ice model.

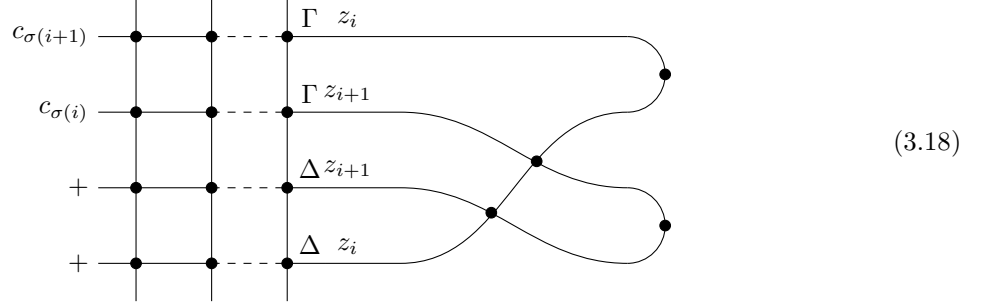
Note that the only admissible configuration of the two R-vertices is given as follows



Therefore we have

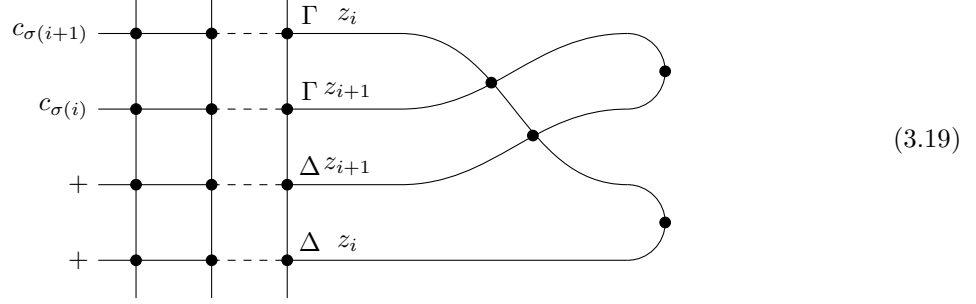
$$Z_1 = R_{\Delta\Delta}(+, +, +, +; z_i, z_{i+1}) R_{\Delta,\Gamma}(+, c_{\sigma(i)}, +, c_{\sigma(i)}; z_i, z_{i+1}) Z(\mathcal{S}_{n,L,\lambda,\sigma,\tau,s_i z}). \quad (3.17)$$

By Theorem 3.1, we can push the two R-vertices to the right without changing the partition function. Namely, we denote by Z_2 the partition function of the following configuration

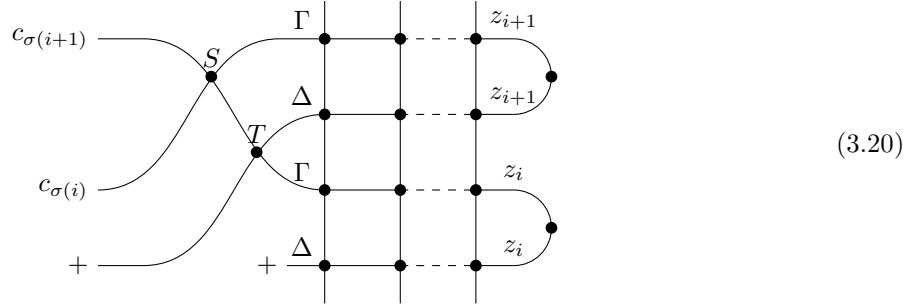


Then we have $Z_1 = Z_2$.

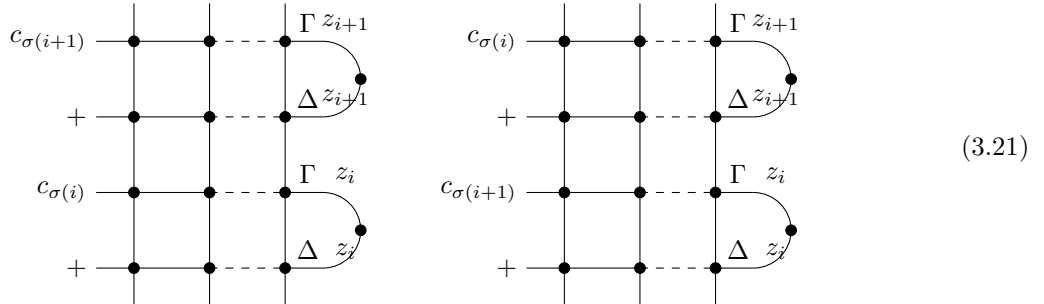
By Theorem 3.3, Z_2 is equal to the partition function of the following configuration



Using Theorem 3.1, we push the two R-vertices back to the left without changing the partition function. Namely, if we denote the partition function of the following configuration by Z_3 , then $Z_3 = Z_2$. Here S is colored stochastic $\Gamma - \Gamma$ vertex of spectral parameters z_{i+1}, z_i , and T is colored stochastic $\Delta - \Gamma$ vertex of spectral parameters z_{i+1}, z_i .



Now we denote by Z_4 and Z_5 the partition functions of the following two configurations.



By considering all possible configurations of S, T , we conclude that

$$Z_3 = R_{\Gamma\Gamma}(c_{\sigma(i)}, c_{\sigma(i+1)}, c_{\sigma(i+1)}, c_{\sigma(i)}; z_{i+1}, z_i) R_{\Delta\Gamma}(+, c_{\sigma(i)}, +, c_{\sigma(i)}; z_{i+1}, z_i) Z_4 + R_{\Gamma\Gamma}(c_{\sigma(i)}, c_{\sigma(i+1)}, c_{\sigma(i)}, c_{\sigma(i+1)}; z_{i+1}, z_i) R_{\Delta\Gamma}(+, c_{\sigma(i+1)}, +, c_{\sigma(i+1)}; z_{i+1}, z_i) Z_5 \quad (3.22)$$

Now note that

$$Z_4 = Z(\mathcal{S}_{n,L,\lambda,\sigma,\tau,z}), \quad (3.23)$$

$$Z_5 = Z(\mathcal{S}_{n,L,\lambda,\sigma s_i,\tau,z}). \quad (3.24)$$

Therefore we have

$$\begin{aligned} & R_{\Delta\Delta}(+, +, +, +; z_i, z_{i+1}) R_{\Delta\Gamma}(+, c_{\sigma(i)}, +, c_{\sigma(i)}; z_i, z_{i+1}) Z(\mathcal{S}_{n,L,\lambda,\sigma,\tau,s_i z}) \\ &= R_{\Gamma\Gamma}(c_{\sigma(i)}, c_{\sigma(i+1)}, c_{\sigma(i+1)}, c_{\sigma(i)}; z_{i+1}, z_i) R_{\Delta\Gamma}(+, c_{\sigma(i)}, +, c_{\sigma(i)}; z_{i+1}, z_i) Z(\mathcal{S}_{n,L,\lambda,\sigma,\tau,z}) \\ &+ R_{\Gamma\Gamma}(c_{\sigma(i)}, c_{\sigma(i+1)}, c_{\sigma(i)}, c_{\sigma(i+1)}; z_{i+1}, z_i) R_{\Delta\Gamma}(+, c_{\sigma(i+1)}, +, c_{\sigma(i+1)}; z_{i+1}, z_i) Z(\mathcal{S}_{n,L,\lambda,\sigma s_i,\tau,z}) \end{aligned} \quad (3.25)$$

Using the Boltzmann weights for colored R-matrices and simplifying the expressions, we obtain the conclusion of the theorem. \square

3.5.2 Proof of Theorem 3.5

The proof of Theorem 3.5 is based on the following idea. First note that only one color (other than c_0), denoted by R , may appear in the $2n$ th row. So we can simultaneously switch $+$ and R in the $2n$ th row and change Boltzmann weights in a similar way as in the uncolored case. The recursive relation is then derived from the Yang-Baxter equation (Theorem 3.1) and a variant of the fish relation using two auxiliary caps given by equation (3.32).

Proof. We note that all the boundary edges on the top of the rectangular lattice carry the $+$ spin, and there are only two possible colors $c_{\sigma(n)}$ and $+$ in the $2n$ th row. We write $R := c_{\sigma(n)}$ hereafter to simplify the notations. Therefore, only the three states in Figure 26 are involved in the $2n$ th row of the lattice. Moreover, only the two states in Figure 27 are involved in the cap connecting the last two rows.

1	qz_n	$1 - qz_n$

Figure 26: Boltzmann weights involved in the $2n$ th row

	1	1
Boltzmann weight		

Figure 27: Boltzmann weights involved for the cap connecting the last two rows

Now for each admissible state we change the color in the $2n$ th row from $+$ to R and from R to $+$ (note that no other colors are involved in the $2n$ th row for an admissible state). Meanwhile we change the Boltzmann weights for the vertices in the $2n$ th row into the ones presented in Figure 28, and change the Boltzmann weights for the caps connecting the last two rows into those in Figure 29. Note that in the original configuration, if the colored path entering from the left of the $2n$ th row doesn't go through the cap connecting the last two rows, then one c_1 pattern is involved (and no c_2 pattern is involved); otherwise neither c_1 nor c_2 is involved. Thus noting the changed Boltzmann weights for the cap, we can deduce that if we denote by Z_1 the partition function of the new system, then

$$Z_1 = \left(\frac{1}{qz_n}\right)^L Z(\mathcal{S}_{n,L,\lambda,\sigma,\tau,z}). \quad (3.26)$$

Note that the new weight for the $2n$ th row is a colored stochastic Δ vertex with spectral parameter $\frac{1}{z'_n}$. Now we attach an R-vertex (colored stochastic $\Delta - \Delta$ vertex with spectral parameters $\frac{1}{z'_n}$ and z_n) to the left

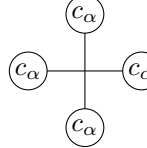
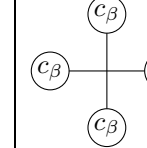
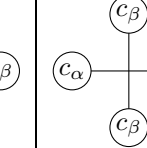
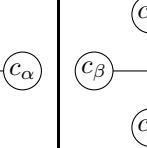
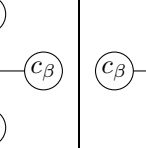
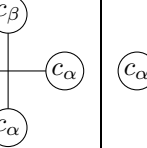
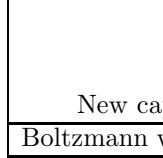
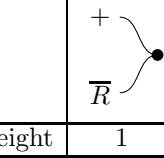
a_1/a_2	a_1/a_2	b_1	b_2	d_1	d_2
					
1	1	$\frac{1}{z_n}$	$\frac{1}{qz_n}$	$1 - \frac{1}{z_n}$	$1 - \frac{1}{qz_n}$

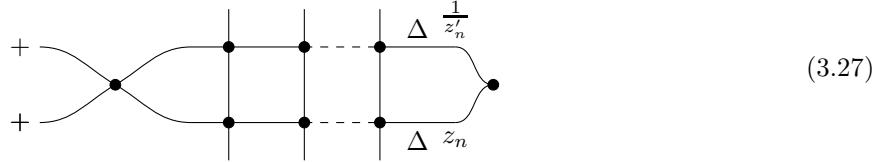
Figure 28: New Boltzmann weights for the $2n$ th row, where $\alpha < \beta$

	
New cap	$+\overline{R}$

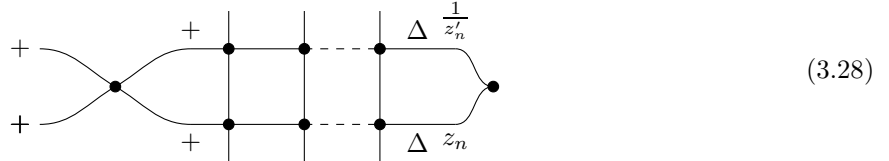
	
Boltzmann weight	1 -1

Figure 29: New Boltzmann weights for the cap connecting the last two rows

boundary of the last two rows of the new system:

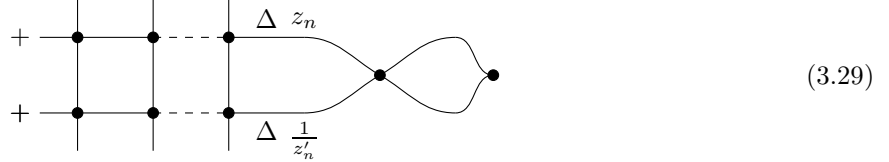


Note that the only admissible configuration of the R-matrix is given by



Therefore, the partition function of the above system is equal to Z_1 .

By Theorem 3.1, we can push the R-vertex to the right without changing the partition function. That is, the partition function of the above system is equal to the partition function of the following



We introduce two types of auxiliary caps C_1 and C_2 . The weights for these caps are shown in Figures 30-31.

Now let $Z(I_1(\epsilon_1, \epsilon_2))$ be the partition function of the following system for every choice of $\epsilon_1, \epsilon_2 \in \{c_{\bar{n}}, \dots, c_n\}$ (where the R-vertex is the one we used above, and the cap weights are given by those in Figure 29).

$$I_1(\epsilon_1, \epsilon_2) = \begin{array}{c} \epsilon_1 \\ \epsilon_2 \end{array} \quad (3.30)$$

New cap	$\begin{array}{c} + \\ \swarrow \\ \overline{R} \end{array} \bullet C_1$	$\begin{array}{c} R \\ \swarrow \\ + \end{array} \bullet C_1$
Boltzmann weight	1	-1

Figure 30: Boltzmann weights for the cap C_1

New cap	$\begin{array}{c} + \\ \swarrow \\ R \end{array} \bullet C_2$	$\begin{array}{c} \overline{R} \\ \swarrow \\ + \end{array} \bullet C_2$
Boltzmann weight	-1	1

Figure 31: Boltzmann weights for the cap C_2

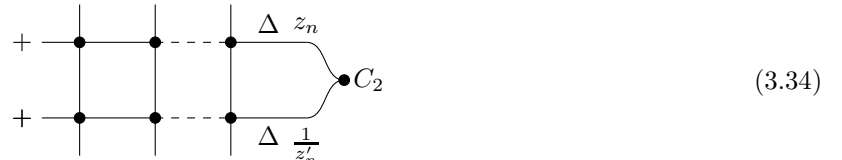
Also denote by $Z(I_2(\epsilon_1, \epsilon_2)), Z(I'_2(\epsilon_1, \epsilon_2))$ the partition functions of the following two systems for every choice of $\epsilon_1, \epsilon_2 \in \{c_{\overline{n}}, \dots, c_n\}$.

$$I_2(\epsilon_1, \epsilon_2) = \begin{array}{c} \epsilon_1 \\ \swarrow \\ \bullet C_1 \end{array} \quad \text{and} \quad I'_2(\epsilon_1, \epsilon_2) = \begin{array}{c} \epsilon_1 \\ \swarrow \\ \epsilon_2 \\ \bullet C_2 \end{array} \quad (3.31)$$

Then we can check that for any ϵ_1, ϵ_2 ,

$$Z(I_1(\epsilon_1, \epsilon_2)) = \frac{(qz_n - 1)(1 - z'_n)}{qz_n + z'_n - (q + 1)} Z(I_2(\epsilon_1, \epsilon_2)) + \frac{q(z_n z'_n - 1)}{qz_n + z'_n - (q + 1)} Z(I'_2(\epsilon_1, \epsilon_2)) \quad (3.32)$$

Thus if we denote by Z_2, Z'_2 the partition functions of the following two configurations, then



$$Z_1 = \frac{(qz_n - 1)(1 - z'_n)}{qz_n + z'_n - (q + 1)} Z_2 + \frac{q(z_n z'_n - 1)}{qz_n + z'_n - (q + 1)} Z'_2. \quad (3.35)$$

Finally we compute Z_2, Z'_2 . For Z_2 , we change the Boltzmann weights of the 2nth row to the weights in Figure 32. We also change the Boltzmann weight of the cap to those in Figure 33 (call it C'_1). It can be checked that the partition function doesn't change.

Now note that the top boundary edges all carry the + spin, we use the previous argument (changing R to + and + to R , and changing Boltzmann weights accordingly) to show that Z_2 is equal to $(\frac{z_n}{q})^L$ times the

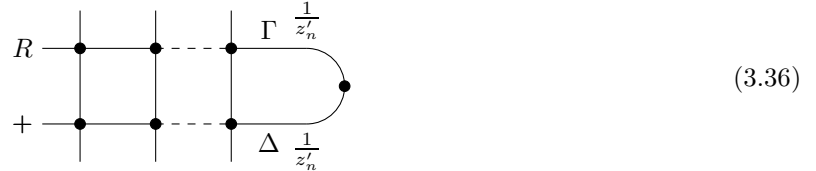
a_1/a_2	a_1/a_2	b_1	b_2	d_1	d_2
1	1	z'_n	$\frac{1}{q}z'_n$	$z'_n - 1$	$\frac{1}{q}z'_n - 1$

Figure 32: New Boltzmann weights for the $2n$ th row, where $\alpha < \beta$: for computing Z_2

New cap		
Boltzmann weight	1	1

Figure 33: Boltzmann weights for the cap C'_1

partition function of the following system, which is $Z(\mathcal{S}_{n,L,\lambda,\sigma,\tau,s_n z})$.

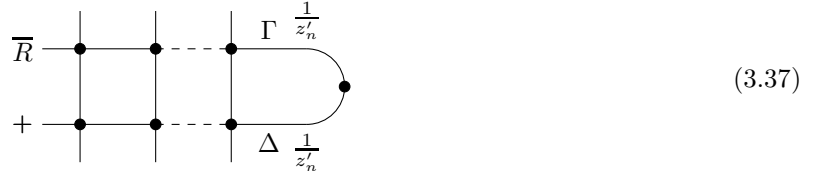


For Z'_2 , we change the Boltzmann weights of the $2n$ th row to the weights in Figure 32. We also change the Boltzmann weights of the cap to those in Figure 34 (call it C'_2). It can be checked that the partition function changes by a factor of -1 . Now note again that the top boundary edges all carry the $+$ spin, we

New cap		
Boltzmann weight	1	1

Figure 34: Boltzmann weights for the cap C'_2

use the previous argument (this time we change \bar{R} to $+$ and $+$ to \bar{R} , and change the Boltzmann weights accordingly) to show that Z'_2 is equal to $-(z'_n)^L$ times the partition function of the following system, which is $Z(\mathcal{S}_{n,L,\lambda,\sigma s_n, \tau, s_n z})$.



Therefore we conclude that

$$\begin{aligned} \left(\frac{1}{z_n}\right)^L Z(\mathcal{S}_{n,L,\lambda,\sigma,\tau,z}) &= \frac{(qz_n - 1)(1 - z'_n)}{z'_n + qz_n - (q + 1)} z'^L_n Z(\mathcal{S}_{n,L,\lambda,\sigma,\tau,s_n z}) \\ &\quad - \frac{q(z_n z'_n - 1)}{qz_n + z'_n - (q + 1)} q^L z'^L_n Z(\mathcal{S}_{n,L,\lambda,\sigma s_n, \tau, s_n z}). \end{aligned} \quad (3.38)$$

By rearranging and changing z to $s_n z$ we reach the conclusion of the theorem. \square

3.6 Relation to Demazure-Lusztig operators of type C

The recursive relations for colored stochastic symplectic ice shown in Section 3.5 are related to Demazure-Lusztig operators of type C. We explain this connection in this section.

Viewed as operators on rational functions of $u = (u_1, \dots, u_n)$, Demazure-Lusztig operators of type C can be given as follows (see [14],[27] for details). For $1 \leq i \leq n - 1$, define

$$s_i(u_1, \dots, u_n) = (u_1, \dots, u_{i+1}, u_i, \dots, u_n), \quad (3.39)$$

that is, s_i transposes u_i and u_{i+1} . Also define

$$s_n(u_1, \dots, u_n) = (u_1, \dots, u_{n-1}, u_n^{-1}). \quad (3.40)$$

For every $1 \leq i \leq n$, and any rational function $f(u)$ of u , we let

$$s_i f(u) := f(s_i u). \quad (3.41)$$

Then Demazure-Lusztig operators (with parameter v) $\mathcal{L}_{i,v}$ are given by

$$\mathcal{L}_{i,v}(f) = \frac{1-v}{u^{\alpha_i} - 1} f + \frac{v u^{\alpha_i} - 1}{u^{\alpha_i} - 1} s_i(f), \quad (3.42)$$

where $\{\alpha_i\}$ are the simple roots of type C_n , that is, $\alpha_i = \epsilon_i - \epsilon_{i+1}$ for $1 \leq i \leq n - 1$ and $\alpha_n = 2\epsilon_n$. Here ϵ_i is the n -dimensional vector such that its i th coordinate is 1 and the other coordinates are 0, for every $1 \leq i \leq n$.

We also let $\hat{\mathcal{L}}_{i,v} = \mathcal{L}_{i,v} - v + 1$. Note that from the quadratic relation for $\mathcal{L}_{i,v}$,

$$\mathcal{L}_{i,v}^2 = (v - 1)\mathcal{L}_{i,v} + v, \quad (3.43)$$

we obtain

$$\hat{\mathcal{L}}_{i,v} \mathcal{L}_{i,v} = v. \quad (3.44)$$

In order to relate the recursive relations to Demazure-Lusztig operator of type C, we make the following change of variables. We let

$$u_i = \frac{1 - qz_i}{1 - z_i} \quad (3.45)$$

for every $1 \leq i \leq n$. Then we have

$$z_i = \frac{1 - u_i}{q - u_i}, \quad (3.46)$$

$$z'_i = \frac{1 - qu_i}{1 - u_i}. \quad (3.47)$$

Under this change of variables, we obtain that for every $1 \leq i \leq n - 1$,

$$A(q, z, i) = \frac{(q - 1)u_i}{u_i - u_{i+1}}, \quad (3.48)$$

$$B(q, z, i) = \frac{qu_i - u_{i+1}}{u_i - u_{i+1}}, \quad (3.49)$$

$$C(q, z) = \frac{1 - q}{q(1 - u_n^2)}, \quad (3.50)$$

$$D(q, z) = \frac{1 - qu_n^2}{q(1 - u_n^2)}, \quad (3.51)$$

where $A(q, z, i)$ and $B(q, z, i)$ are as in Theorem 3.4, and $C(q, z)$ and $D(q, z)$ are as in Theorem 3.5.

Now we let

$$Z(\tilde{\mathcal{S}}_{n, L, \lambda, \sigma, \tau, u}) = Z(\mathcal{S}_{n, L, \lambda, \sigma, \tau, z}) \frac{q^{\sum_{i=1}^n (n-i)1_{\sigma(i)>0} + (L+1)\sum_{i=1}^n 1_{\sigma(i)<0}}}{\prod_{i=1}^n z_i^L} \quad (3.52)$$

as a function of $u = (u_1, \dots, u_n)$. Then Theorems 3.4 and 3.5 translate into the following

Theorem 3.6. *For $1 \leq i \leq n-1$, if $\sigma(i+1) > \sigma(i)$ we have*

$$Z(\tilde{\mathcal{S}}_{n, L, \lambda, \sigma s_i, \tau, u}) = \hat{\mathcal{L}}_{i, q}(Z(\tilde{\mathcal{S}}_{n, L, \lambda, \sigma, \tau, u})). \quad (3.53)$$

Moreover, if $\sigma(n) > 0$, we have

$$Z(\tilde{\mathcal{S}}_{n, L, \lambda, \sigma s_n, \tau, u}) = -\mathcal{L}_{n, q}(Z(\tilde{\mathcal{S}}_{n, L, \lambda, \sigma, \tau, u})). \quad (3.54)$$

4 Another colored model for stochastic symplectic ice

In this section, we present a different colored model for the stochastic symplectic ice. In this model, the set of colors is $\{c_1, \dots, c_n\}$. We also denote by $c_0 = +$.

The model and related Boltzmann weights are introduced in Section 4.1. Then the Boltzmann weights for the R-matrices are introduced in Section 4.2, and the Yang-Baxter equation is proved there. Finally in Section 4.3 the reflection equation is introduced, based on which the recursive relations of the partition function are derived.

4.1 The colored model

We introduce the new colored stochastic symplectic ice in this section. The set of colors for this model is given by $\{c_1, \dots, c_n\}$.

In this model, there are also two types of vertices termed ‘‘colored stochastic Γ vertex’’ and ‘‘colored stochastic Δ vertex’’. The model depends on n spectral parameters z_1, \dots, z_n and a deformation parameter q , and we take

$$z'_i = q + 1 - \frac{1}{z_i}.$$

The Boltzmann weights for these two types of vertices are listed in Figures 35-36.

a_1/a_2	a_2/a_2	b_1	b_2	c_1	c_2
1	1	z_i	qz_i	$1 - qz_i$	$1 - z_i$

Figure 35: Boltzmann weights for colored stochastic Γ vertex with spectral parameter z_i , where $\alpha < \beta$

a_1/a_2	a_1/a_2	b_1	b_2	d_1	d_2
1	1	z'_i	$\frac{1}{q}z'_i$	$1 - z'_i$	$1 - \frac{1}{q}z'_i$

Figure 36: Boltzmann weights for colored stochastic Δ vertex with spectral parameter z_i , where $\alpha < \beta$ and $z'_i = q + 1 - \frac{1}{z_i}$

The basic set-up of the new model is similar to that of the colored model given in Section 3. The difference lies in the assignment of boundary conditions: now we specify two permutations σ, τ from the symmetric group S_n , assigning the color $c_{\tau(i)}$ to each column labeled $\lambda_i + n + 1 - i$ for $1 \leq i \leq n$ at the bottom, and assigning the color $c_{\sigma(i)}$ to the left boundary of the i th row of colored stochastic Γ vertex. The Boltzmann weights for the caps are given in Figure 37.

Cap		
	Boltzmann weight	1

Figure 37: Boltzmann weights of the caps for the new colored model, where $\alpha \in \{1, 2, \dots, n\}$

Hereafter we denote by $\mathcal{U}_{n,L,\lambda,\sigma,\tau,z}$ the collection of admissible configurations with the corresponding data. We also denote by $Z(\mathcal{U}_{n,L,\lambda,\sigma,\tau,z})$ the partition function. We assume that $L \geq \lambda_1 + n$, too.

We note that the Boltzmann weights for this model are also stochastic, which allows a probabilistic interpretation of the model when the condition (2.1) is satisfied. The colored model can be similarly interpreted as stochastic dynamics as the colored model given in Section 3. The main difference is that in this model, the particles don't change color when they are reflected at the caps.

4.2 The R-matrix and the Yang-Baxter equation

For this model, we also find three sets of Yang-Baxter equations. The corresponding R-matrices are termed “colored stochastic $\Gamma - \Gamma$ vertex”, “colored stochastic $\Delta - \Gamma$ vertex” and “colored stochastic $\Delta - \Delta$ vertex”, too. The Boltzmann weights for the three types of R-matrices are given in Figures 38-40.

1	1	$\frac{z_i - z_j}{1 - (q+1)z_j + qz_i z_j}$	$\frac{q(z_i - z_j)}{1 - (q+1)z_j + qz_i z_j}$	$\frac{(1 - qz_i)(1 - z_j)}{1 - (q+1)z_j + qz_i z_j}$	$\frac{(1 - z_i)(1 - qz_j)}{1 - (q+1)z_j + qz_i z_j}$

Figure 38: Boltzmann weights for colored stochastic $\Gamma - \Gamma$ vertex with spectral parameters z_i and z_j : where $\alpha < \beta$

1	1	$\frac{z'_i + qz_j - (q+1)z'_i z_j}{1 - z'_i z_j}$	$\frac{q^{-1}z'_i + z_j - (1+q^{-1})z'_i z_j}{1 - z'_i z_j}$	$\frac{(1-z'_i)(1-qz_j)}{1 - z'_i z_j}$	$\frac{(1-q^{-1}z'_i)(1-z_j)}{1 - z'_i z_j}$

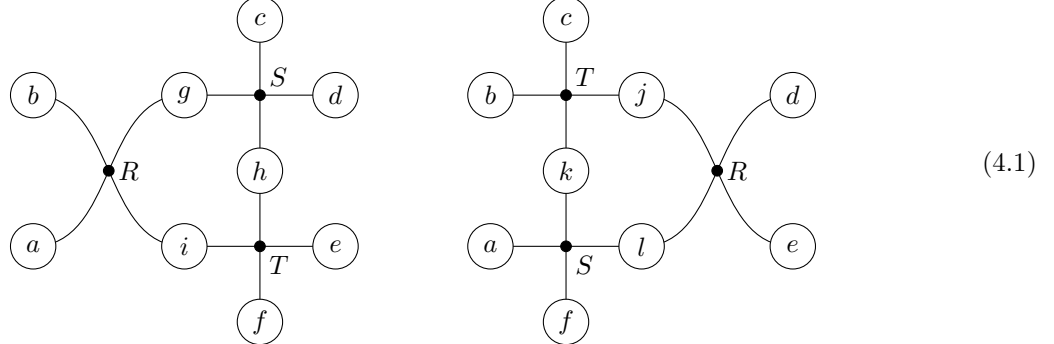
Figure 39: Boltzmann weights for colored stochastic $\Delta - \Gamma$ vertex with spectral parameters z_i and z_j : where $\alpha < \beta$

1	1	$\frac{z'_j - z'_i}{q - (q+1)z'_i + z'_i z'_j}$	$\frac{q(z'_j - z'_i)}{q - (q+1)z'_i + z'_i z'_j}$	$\frac{(1-z'_i)(q-z'_j)}{q - (q+1)z'_i + z'_i z'_j}$	$\frac{(1-z'_j)(q-z'_i)}{q - (q+1)z'_i + z'_i z'_j}$

Figure 40: Boltzmann weights for colored stochastic $\Delta - \Delta$ vertex with spectral parameters z_i and z_j : where $\alpha < \beta$

The following theorem gives the three sets of Yang-Baxter equations for the colored stochastic symplectic ice.

Theorem 4.1. *For any $(X, Y) \in \{(\Delta, \Gamma), (\Gamma, \Gamma), (\Delta, \Delta)\}$ the following holds. Assume that S is colored stochastic X vertex with spectral parameter z_i , T is colored stochastic Y vertex with spectral parameter z_j , and R is colored stochastic $X - Y$ vertex with spectral parameters z_i, z_j . Then the partition functions of the following two configurations are equal for any fixed combination of colors $a, b, c, d, e, f \in \{c_0, \dots, c_n\}$.*

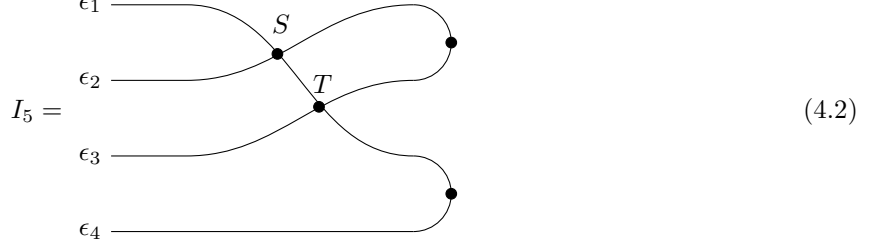


Proof. From conservation of colors for both colored stochastic Γ vertices and colored stochastic Δ vertices (note that the directions of input and output are different for these two types of vertices), it can be checked that at most four distinct colors (including c_0) can appear on the boundary edges in any of the two configurations, and that the color on an inner edge must be one of the colors on boundary edges (only considering admissible configurations). Moreover, the Boltzmann weight of a vertex only depends on the relative order of the colors on its adjacent four edges. Therefore it suffices to check the result for four colors, and there are at most 4^6 possible combinations of boundary colors. These identities are checked using a SAGE program. \square

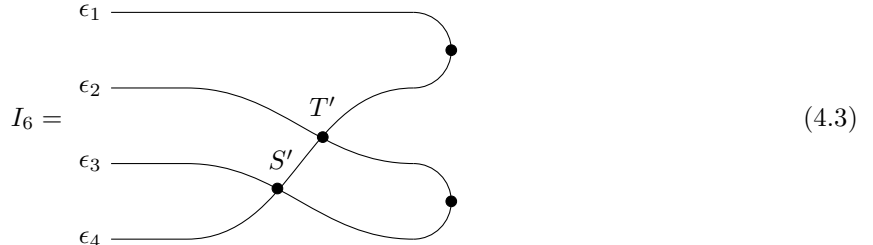
4.3 The reflection equation and recursive relations of the partition function

In the new model, we also have the reflection equation:

Theorem 4.2. *Assume that S is colored stochastic $\Gamma - \Gamma$ vertex of spectral parameters z_i, z_j , T is colored stochastic $\Delta - \Gamma$ vertex of spectral parameters z_i, z_j , S' is colored stochastic $\Delta - \Delta$ vertex of spectral parameters z_j, z_i , and T' is colored stochastic $\Delta - \Gamma$ vertex of spectral parameters z_j, z_i . Denote by $Z(I_5(\epsilon_1, \epsilon_2, \epsilon_3, \epsilon_4))$ the partition function of the following configuration with fixed combination of colors $\epsilon_1, \epsilon_2, \epsilon_3, \epsilon_4 \in \{c_0, \dots, c_n\}$.*



Also denote by $Z(I_6(\epsilon_1, \epsilon_2, \epsilon_3, \epsilon_4))$ the partition function of the following configuration with fixed combination of colors $\epsilon_1, \epsilon_2, \epsilon_3, \epsilon_4 \in \{c_0, \dots, c_n\}$.



Then for any fixed combination of colors $\epsilon_1, \epsilon_2, \epsilon_3, \epsilon_4 \in \{c_0, \dots, c_n\}$, we have

$$Z(I_5(\epsilon_1, \epsilon_2, \epsilon_3, \epsilon_4)) = Z(I_6(\epsilon_1, \epsilon_2, \epsilon_3, \epsilon_4)). \quad (4.4)$$

Proof. From conservation of colors for the R-matrix and the cap weights, we can deduce that for any admissible state of I_5 or I_6 , each color must appear for an even number of times in $\{\epsilon_1, \epsilon_2, \epsilon_3, \epsilon_4\}$, and that the color of an inner edge must be one of the colors of $\{\epsilon_1, \epsilon_2, \epsilon_3, \epsilon_4\}$. From this we can further deduce that at most two colors can appear in $\{\epsilon_1, \epsilon_2, \epsilon_3, \epsilon_4\}$ in any admissible state of I_5 or I_6 . Moreover, we note that the Boltzmann weight for the R-matrix only depends on the relative order of colors on its four adjacent edges. Therefore it suffices to check the relation for three colors $\{c_0, c_1, c_2\}$. There are at most 3^4 combinations of $(\epsilon_1, \epsilon_2, \epsilon_3, \epsilon_4)$ for this case. These identities have been checked using a SAGE program. \square

Based on the Yang-Baxter equation (Theorem 4.1) and the reflection equation (Theorem 4.2), we can establish the following theorem on the recursive relations for the partition function $Z(\mathcal{U}_{n,L,\lambda,\sigma,\tau,z})$. The proof of Theorem 4.3 is similar to that of Theorem 3.4 and we omit it.

Theorem 4.3. *Assume that $1 \leq i \leq n-1$ and $\sigma(i+1) > \sigma(i)$. Let s_i be the transposition $(i, i+1)$ in the symmetric group S_n , and let $s_i z$ be the vector obtained from z by interchanging z_i, z_{i+1} . Then the partition function of the new colored model satisfies the following recursive relation:*

$$Z(\mathcal{U}_{n,L,\lambda,\sigma s_i, \tau, z}) = -A(q, z, i)Z(\mathcal{U}_{n,L,\lambda,\sigma, \tau, z}) + B(q, z, i)Z(\mathcal{U}_{n,L,\lambda,\sigma, \tau, s_i z}), \quad (4.5)$$

where

$$A(q, z, i) = \frac{(1 - z_{i+1})(1 - qz_i)}{z_{i+1} - z_i}, \quad (4.6)$$

and

$$B(q, z, i) = \frac{1 - (q+1)z_i + qz_i z_{i+1}}{z_{i+1} - z_i}. \quad (4.7)$$

References

- [1] BAXTER, R. The inversion relation method for some two-dimensional exactly solved models in lattice statistics. *Journal of Statistical Physics* 28, 1 (1982), 1–41.
- [2] BAXTER, R. J. *Exactly solved models in statistical mechanics*. Elsevier, 2016.
- [3] BORODIN, A. On a family of symmetric rational functions. *Advances in Mathematics* 306 (2017), 973–1018.
- [4] BORODIN, A., AND PETROV, L. Integrable probability: stochastic vertex models and symmetric functions. In *Stochastic processes and random matrices* (2017), pp. 26–131.
- [5] BORODIN, A., AND WHEELER, M. Coloured stochastic vertex models and their spectral theory. *arXiv preprint arXiv:1808.01866* (2018).
- [6] BRUBAKER, B., BUCIUMAS, V., AND BUMP, D. A Yang-Baxter equation for metaplectic ice. *arXiv preprint arXiv:1604.02206* (2016).
- [7] BRUBAKER, B., BUCIUMAS, V., BUMP, D., AND GUSTAFSSON, H. Colored vertex models and Iwahori Whittaker functions. *arXiv preprint arXiv:1906.04140* (2019).
- [8] BRUBAKER, B., BUCIUMAS, V., BUMP, D., AND GUSTAFSSON, H. Metaplectic Iwahori Whittaker functions and supersymmetric lattice models. *arXiv preprint arXiv:2012.15778* (2020).
- [9] BRUBAKER, B., BUCIUMAS, V., BUMP, D., AND GUSTAFSSON, H. P. Vertex operators, solvable lattice models and metaplectic Whittaker functions. *Communications in Mathematical Physics* 380, 2 (2020), 535–579.
- [10] BRUBAKER, B., BUCIUMAS, V., BUMP, D., AND GUSTAFSSON, H. P. Colored five-vertex models and Demazure atoms. *Journal of Combinatorial Theory, Series A* 178 (2021), 105354.
- [11] BRUBAKER, B., BUMP, D., CHINTA, G., FRIEDBERG, S., AND GUNNELLS, P. E. Metaplectic ice. In *Multiple Dirichlet series, L-functions and automorphic forms*. Springer, 2012, pp. 65–92.
- [12] BRUBAKER, B., BUMP, D., CHINTA, G., AND GUNNELLS, P. Crystals of type B and metaplectic Whittaker functions. *preprint* (2010).
- [13] BRUBAKER, B., BUMP, D., AND FRIEDBERG, S. Schur polynomials and the Yang-Baxter equation. *Communications in mathematical physics* 308, 2 (2011), 281.
- [14] BRUBAKER, B., BUMP, D., AND LICATA, A. Whittaker functions and Demazure operators. *Journal of Number Theory* 146 (2015), 41–68.
- [15] BRUBAKER, B., AND SCHULTZ, A. The six-vertex model and deformations of the Weyl character formula. *Journal of Algebraic Combinatorics* 42, 4 (2015), 917–958.
- [16] BRUBAKER, B., AND SCHULTZ, A. On Hamiltonians for six-vertex models. *Journal of Combinatorial Theory, Series A* 155 (2018), 100–121.
- [17] BUCIUMAS, V., AND SCRIMSHAW, T. Quasi-solvable lattice models for Sp_{2n} and SO_{2n+1} Demazure atoms and characters. *arXiv preprint arXiv:2101.08907* (2021).
- [18] CORWIN, I., AND PETROV, L. Stochastic higher spin vertex models on the line. *Communications in Mathematical Physics* 343, 2 (2016), 651–700.
- [19] GRAY, N. Metaplectic ice for Cartan type C. *arXiv preprint arXiv:1709.04971* (2017).

- [20] HAMEL, A., AND KING, R. Symplectic shifted tableaux and deformations of Weyl's denominator formula for $sp(2n)$. *Journal of Algebraic Combinatorics* 16, 3 (2002), 269–300.
- [21] HAMEL, A., AND KING, R. U-turn alternating sign matrices, symplectic shifted tableaux and their weighted enumeration. *Journal of Algebraic Combinatorics* 21, 4 (2005), 395–421.
- [22] IVANOV, D. Symplectic ice. In *Multiple Dirichlet series, L-functions and automorphic forms*. Springer, 2012, pp. 205–222.
- [23] KUPERBERG, G. Another proof of the alternative-sign matrix conjecture. *International Mathematics Research Notices* 1996, 3 (1996), 139–150.
- [24] KUPERBERG, G. Symmetry classes of alternating-sign matrices under one roof. *Annals of mathematics* (2002), 835–866.
- [25] MOTEGI, K. Dual wavefunction of the symplectic ice. *Reports on Mathematical Physics* 80, 3 (2017), 391–414.
- [26] MOTEGI, K., SAKAI, K., AND WATANABE, S. Quantum inverse scattering method and generalizations of symplectic Schur functions and Whittaker functions. *Journal of Geometry and Physics* 149 (2020), 103571.
- [27] PUSKAS, A. *Demazure-Lusztig operators and metaplectic Whittaker functions on covers of the general linear group*. PhD thesis, Columbia University, 2014.
- [28] WHEELER, M., AND ZINN-JUSTIN, P. Littlewood–Richardson coefficients for Grothendieck polynomials from integrability. *Journal für die reine und angewandte Mathematik* 2019, 757 (2019), 159–195.